RSC Advances

REVIEW

View Article Online
View Journal | View Issue

Cite this: *RSC Adv.*, 2025, **15**, 7995

Research on performance constraints and electrolyte optimization strategies for lithium-ion batteries at low temperatures

Changlin Liu,[a] Lizhi Sheng *[ab] and Lili Jiang *[c]

Lithium-ion batteries (LIBs) are extensively utilized in electronic devices, electric vehicles, and energy storage systems to meet the growing energy demand, due to their high energy density, extended lifespan, and absence of the memory effect. However, their high performance is significantly diminished at low temperatures. Recent research indicates that the low-temperature performance of LIBs is constrained by the sluggish diffusion of Li^+ in the electrolyte, across the interfaces, and within the electrodes. At lower temperatures, the rise in electrolyte viscosity results in a slower ion transport rate, which is a key factor affecting battery performance. The electrolyte primarily consists of lithium salts, solvents, and additives, and improvements in these three aspects are crucial for the creation of electrolytes with excellent low-temperature performance. This review systematically introduces the factors responsible for the decline in LIBs performance at low temperatures, including reduced ionic conductivity in the electrolyte, increased Li^+ desolvation energy in the electrolyte, slow transfer kinetics at the interface, on the anode significant lithium plating and dendrite formation, and slow Li^+ diffusion within the electrode material. Advancements in research on lithium salts, solvents, additives, and novel electrolytes are methodically presented, comprising localized high-concentration electrolytes, weakly solvating electrolytes, liquefied gas electrolytes, and polymer electrolytes. Finally, the challenges that must be addressed in current low-temperature LIBs are identified, and potential future developments in this field are anticipated.

Received 2nd December 2024
Accepted 7th March 2025

DOI: 10.1039/d4ra08490j

rsc.li/rsc-advances

1. Introduction

As global energy demand continues to rise, the excessive use of fossil fuels poses a significant threat to environmental sustainability. Environmental issues such as global warming and the depletion of natural resources, which are linked to fossil fuels, have attracted widespread attention. In response to these challenges, the scientific community is actively researching efficient energy systems to replace traditional internal combustion engines. Lithium-ion batteries (LIBs) have garnered considerable attention in recent years as a potential alternative energy source. LIBs have successfully become the leading power source for portable electronics over the past few decades and are now widely used in electric vehicles, with the potential to become a beneficial substitute in reducing fossil fuel dependency and promoting sustainable energy development in the future.[1–4] LIBs possess advantages such as high energy density, extended cycle life, and no memory effect.[5,6] However, they exhibit significant sensitivity to temperature fluctuations. Their operating temperature range is relatively narrow, with discharge temperatures limited to −20 °C to 50 °C and charging temperatures limited to 0 °C to 45 °C.[7] For example, in regions with high altitudes, high elevations, or extreme latitudes, the performance of LIBs is particularly affected by low temperatures. Another field where low-temperature environments pose challenges for LIB applications is aerospace, where temperatures on Mars can drop to −120 °C.[8] Especially during charging under low-temperature conditions, lithium dendrites may form on the anode, potentially piercing the separator and causing internal short circuits within the battery. This phenomenon can lead to violent reactions in the electrolyte, generating excessive heat and gas, increasing internal pressure, and even causing severe safety issues such as fires or explosions.[9,10] Therefore, in addressing the practical requirements of LIBs, it is essential not only to pursue higher energy density but also to consider a broader operating temperature range and reliable safety measures.

Temperature is a vital aspect of determining the stability and safety of LIBs. Currently, commercial LIBs utilizing ethylene carbonate (EC) and graphite anodes perform poorly at low

[a]College of Materials Science and Engineering, Beihua University, Jilin, 132013, P. R. China. E-mail: shengli_zhi@126.com
[b]Department of Materials Science and Engineering, National University of Singapore, Singapore, 117574, Singapore
[c]Key Laboratory for Special Functional Materials in Jilin Provincial Universities, Jilin Institute of Chemical Technology, Jilin, 132022, P. R. China. E-mail: jianglidipper@126.com

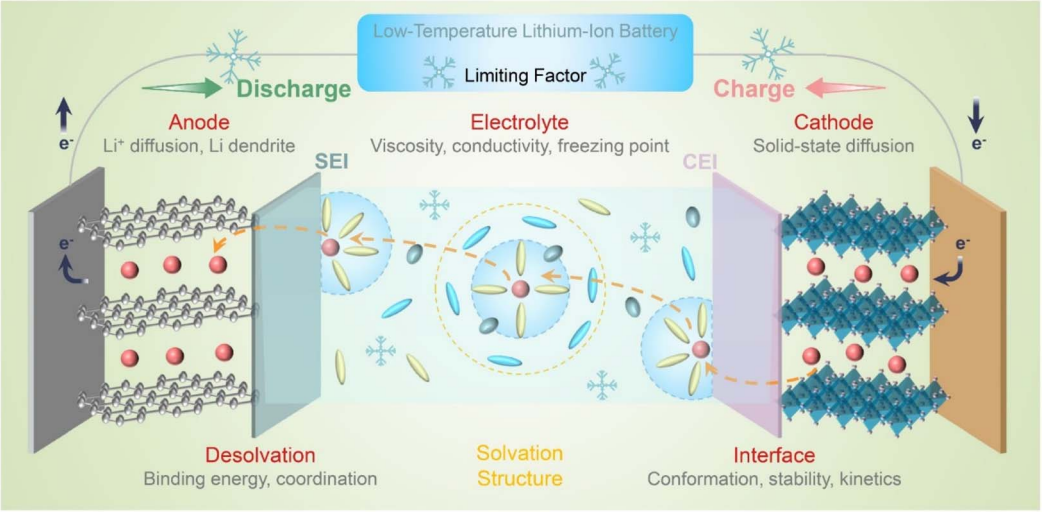

Fig. 1 Limitations encountered by lithium-ion batteries in low-temperature environments.

temperatures (Fig. 1),[11] primarily due to three factors: (1) in low-temperature environments, the ionic conductivity of liquid electrolytes decreases significantly, and viscosity increases;[12,13] (2) electrochemical impedance increases, particularly charge transfer impedance (R_{ct}) and solid electrolyte interface (SEI) impedance (R_{SEI}). At low temperatures, R_{ct} and R_{SEI} account for the majority of the total impedance of LIBs, significantly reducing the desolvation rate of Li^+ in the electrolyte and the diffusion speed at the electrolyte–electrode interface;[14–17] (3) the migration and diffusion rates of Li^+ in electrode materials slow down considerably at low temperatures.[18] The combined effect of these three factors leads to a marked decline in the performance of LIBs under low-temperature conditions. Moreover, lithium metal deposition on the anode is more likely to occur during low-temperature charging, especially at high rates. This exacerbates the irreversible reactions between lithium metal and the electrolyte, leading to electrolyte disintegration and the formation of additional SEI layers. Subsequently, the SEI on the electrode surface thickens, resulting in higher impedance and greater polarization of the LIBs. These side reactions accelerate the growth of lithium dendrites, which can lead to both decreased LIBs performance and potentially increased safety risks.[19–22] Li *et al.*[23] were the first to introduce low-temperature electron microscopy for observing and non-destructively analyzing the architecture, composition, and morphology of the SEI and lithium dendrite on the anode. This innovative method provides critical support for accurately assessing the repercussions of electrolytes on SEI formation. Given that the Li^+ desolvation process in the electrolyte cannot be directly characterized by instruments, molecular dynamics simulations offer an effective means to deeply analyze the desolvation process along with the solvation structure in the electrolyte.[24,25] To ensure excellent performance of LIBs under low-temperature conditions, developing new electrolytes characterized by low viscosity, rapid Li^+ desolvation rates, high ionic conductivity, and stable SEI formation is imperative.

In this review, we investigate the primary factors responsible for the performance decline of LIBs under low-temperature environments. Our focus is on the analysis of Li^+ transport processes within the electrolyte, at the electrolyte–electrode interface, and throughout the electrode materials, to clarify the factors affecting LIBs' low-temperature performance. Subsequently, it explores methods to boost the performance of LIBs in low-temperature conditions by optimizing the electrolyte system, with a focus on lithium salts, solvents, and additives. Additionally, the review introduces some novel electrolyte systems, encompassing localized high-concentration electrolytes, weakly solvating electrolytes, liquefied gas electrolytes, and solid polymer electrolytes. Finally, it summarizes the challenges of preparing high-performance LIBs electrolytes under low-temperature conditions and discusses the future development directions for LIBs electrolytes.

2. Factors affecting the low-temperature performance of LIBs

As the ambient temperature decreases, there is a sharp drop in ionic conductivity in the electrolyte, resulting in slow Li^+ transfer; increased impedance at the electrolyte–electrode interface and limited desolvation kinetics; and decreased diffusion capacity of Li^+ in the electrode material. These are the main factors for the increased polarization and capacity decay of LIBs in low-temperature environments. In addition, uneven lithium metal deposition occurs on the electrode interface, which triggers excessive decomposition of the local electrolyte, resulting in a thick, organic-rich SEI in LIBs throughout charge and discharge processes, ultimately harming the electrode and exhausting the electrolyte.[8,26–28]

2.1. Li^+ transport in electrolyte

In low-temperature environments, the ionic conductivity of LIBs electrolyte is essential since it determines the Li^+ transport

speed within the electrolyte, further affecting the performance of LIBs in low-temperature environments.[29] To probe the factors influencing ionic conductivity under low-temperature conditions, researchers have used molecular dynamics simulations to identify viscosity as the primary factor affecting ion migration within the electrolyte.[30] The relationship between viscosity and ionic conductivity can be determined through a defined equation. Ionic conductivity, which represents the ability of ions to conduct in the electrolyte, is defined by the following equation:[31]

$$\sigma = \Sigma_i n_i \mu_i Z_i e$$

where σ represents ionic conductivity, n_i is the number of free ions, μ_i is the ion mobility, Z_i is the charge number of the ion, and e is the elementary charge of an electron. The ionic conductivity of the electrolyte, as derived from the equation, is mainly influenced by ion mobility (μ_i), the number of free ions (n_i), and the charge state (Z_i). For the composition of the electrolyte, the number of free ions (n_i) and the charge state (Z_i) remain constant, while ion mobility (μ_i) can be represented as:[31]

$$\mu_i = 1/6\pi\eta r_i$$

where η is the electrolyte viscosity and r_i is the solvated ion radius. From the above formula, it can be seen that the ion mobility has an inverse relationship with the electrolyte viscosity, that is, the ion conductivity is also inversely related to the electrolyte viscosity.

However, the decrease in temperature causes an increase in electrolyte viscosity, which consequently leads to a decline in ionic conductivity (Fig. 2a).[32] The solvation structure within the electrolyte is also subject to temperature variations. As the temperature decreases, the molecular dynamics slow down, making molecular interactions increasingly difficult to disrupt. This phenomenon is reflected in a macroscopic reduction in the volume of the solvated structure. When this volume undergoes significant compression, further reductions become

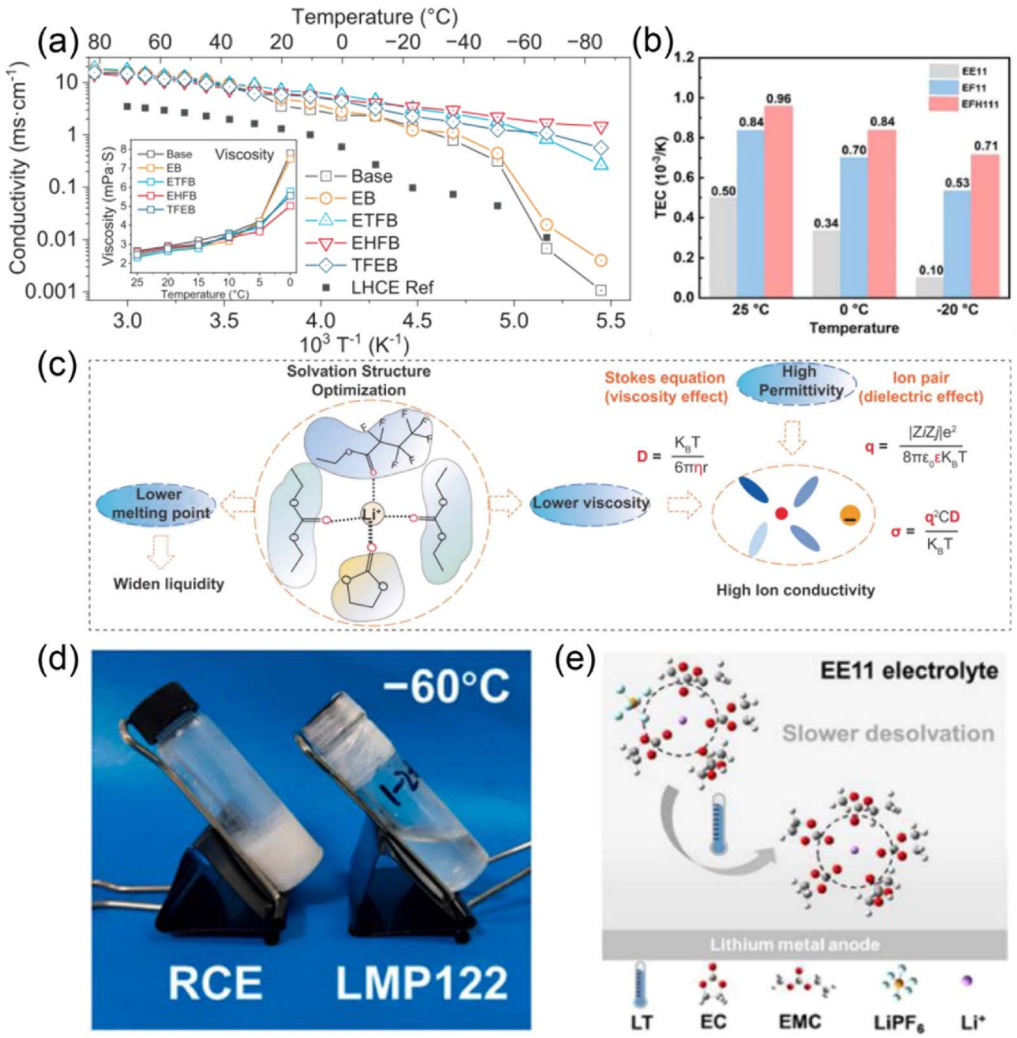

Fig. 2 (a) Curves of electrolyte viscosity and conductivity with temperature. Based on ref. 32. (b) TEC at different temperatures of the electrolyte. Based on ref. 33. (c) The relationship between solvation structure and physical properties of low temperature electrolyte. Based on ref. 32. (d) Optical image of the electrolyte at low temperature. Based on ref. 34. (e) Tendency of solvent in EC-based electrolyte to enter the Li^+ solvated sheath at low temperature. Based on ref. 33.

progressively more difficult. The coefficient of thermal expansion (TEC) quantifies the change in volume associated with each 1 °C variation at a specific temperature and serves as a measure of looseness among the various components within the electrolyte. A higher TEC suggests that the electrolyte can be compressed more easily, implying longer interaction distances between its constituents. Conversely, a lower TEC indicates a denser state characterized by relatively tighter interactions.[35] As temperature decreases, the TEC diminishes due to reduced distances between components, resulting from the strong intermolecular attractions present in commercial electrolytes (Fig. 2b).[33] This reduction not only impacts ion mobility but also increases the energy barriers during desolvation processes, thereby affecting the performance of LIBs under low-temperatures conditions. In addition, the dielectric constant is an important factor influencing electrolyte performance. It indicates the ability of solvent molecules to polarize under an external electric field, reflecting the extent to which a substance responds to such a field. The dielectric constant has a significant influence on the interactions within the solution, which is closely linked to the electrolyte's physicochemical properties.[36] In most cases, electrolytes with higher dielectric constants tend to exhibit higher ionic conductivity. However, the strong intermolecular forces inherent to high-dielectric solvents often lead to increased viscosity. Therefore, achieving optimal ionic conductivity must strike a balance between electrolyte viscosity and dielectric constant (Fig. 2c).[32,37]

Besides ionic conductivity, the freezing point of the electrolyte is another significant factor. Under low-temperature conditions, the freezing point of the electrolyte can influence the performance and reliability of the battery. Most commercial carbonate-based electrolytes possess a high freezing point, which means they solidify at low temperatures, rendering them unsuitable for use in cold environments (Fig. 2d).[34] Therefore, developing electrolytes with low viscosity and low freezing points is particularly crucial.[38] The performance of LIBs is impacted by the desolvation of solvated Li^+ in the electrolyte, especially at extreme temperatures, where the energy barrier for Li^+ desolvation predominates. Desolvation involves the removal of solvent molecules from the solvation shell of Li^+, enabling its insertion into the electrode. This process is highly temperature-dependent. At lower temperatures, the reduced molecular mobility slows down the desolvation kinetics, and the desolvation process of Li^+ becomes kinetically slower. Thus, optimizing the solvation structure of Li^+ by adjusting the coordination strength of Li^+ with solvents or anions is vital.[39] The interactions between electrolyte components, specifically ion–ion and ion–solvent interactions, are classified as electrostatic interactions. According to classical physics principles, these two types of electrostatic forces can be described by the following equations:[33,40,41]

$$U_{\text{ion–ion}} = -1/4\pi\varepsilon \times Z_1 Z_2 e^2/r$$

$$U_{\text{ion–dipole}} = -1/4\pi\varepsilon \times Ze\mu\cos\theta/r^2$$

where U is the electrostatic potential energy, ε is the dielectric constant, r is the distance, μ is the molecule dipole moment of the solvent, and θ is the angle between the ion and the dipole center. In the electrolyte, the solvation structure of Li^+ is primarily governed by the interactions between the anion and the solvent, with the observed equilibrium resulting from these interactions at room temperature. Although a reduction in temperature does not directly affect these interactions, it decreases the overall volume of the electrolyte, thereby shortening the distance r between its components and enhancing the interactions. According to the aforementioned formulas, the ion–ion electrostatic potential energy varies with r^{-1}, while the ion–dipole interaction varies with r^{-2}, indicating that as the temperature decreases, the increase in the latter interaction outpaces that of the former. Consequently, the solvent is likely to dominate in its competition with anions, gaining access to the inner solvation shell of Li^+. Additionally, the dipole moment of the solvent constitutes a vital element in determining the strength of the dipole interaction. EC possessing a higher dipole moment, enhances ion–dipole interactions, further promoting the tendency for solvents to enter the Li^+ solvation sheath at lower temperatures (Fig. 2e). Conversely, when employing solvents with lower dipole moments, anions are more capable of entering the inner solvation layer at low temperature.[33]

Moreover, in lithium-ion battery electrolytes, solvent–solvent interactions have a profound impact on the overall performance of the electrolyte.[42] These interactions not only regulate the arrangement and distribution of solvent molecules but also significantly influence the coordination environment of Li^+ within the solvation structure. Specifically, the dipole–dipole interactions between solvent molecules can modulate the thermodynamic (redox stability) and kinetic (Li^+ desolvation kinetics) properties of the electrolyte by altering the compactness of the solvation shell.[43,44] When strong interactions exist between solvent molecules, they tend to attract each other and form an orderly arrangement, thereby weakening the binding strength between individual solvent molecules and Li^+. This occurs because the solvent molecules are more inclined to interact with each other rather than directly coordinate with Li^+, simplifying the process by which Li^+ detaches from the solvation shell. This effect helps reduce the desolvation energy barrier of Li^+, making it easier for Li^+ to migrate to the electrode surface for electrochemical reactions. By tuning solvent–solvent interactions, the electrolyte's solvation structure can be optimized to facilitate efficient Li^+ desolvation at low temperatures, enhancing battery performance while also preventing Li^+ and solvent co-intercalation into the graphite anode, thereby protecting electrode integrity and improving overall battery stability.[45] Xie *et al.*[46] designed a PC/CPME (PC: propylene carbonate; CPME: cyclopentylmethyl ether) electrolyte and demonstrated that solvent–solvent interactions play a crucial role in regulating the thermodynamic and kinetic properties of the electrolyte. The presence of interactions between PC and CPME was confirmed through two-dimensional nuclear magnetic resonance (NMR), which helps in modulating the Li^+-solvent/anion interactions and the Li^+ solvation structure. This

modulation significantly reduces the desolvation energy barrier of $Li^+(PC)_x(CPME)_y$ clusters and increases the energy gap between the orbitals of $Li^+(PC)_x(CPME)_y$ clusters. Consequently, it achieves rapid Li^+ desolvation kinetics and excellent thermodynamic reduction stability. Additionally, the electrode interfacial behavior is significantly improved, with the graphite||$LiFePO_4$ full cell retaining a high specific capacity of 112 mA h g^{-1} even at 5C.

Building upon these insights, solvent–solvent interactions can be further optimized to enhance the compatibility of electrolytes with alloying anodes such as antimony (Sb), which typically suffer from issues like large volume expansion during cycling.[47,48] While these interactions do not directly reduce the volume expansion of alloying anodes, they help mitigate the associated issues by improving the overall stability of the electrolyte and reducing side reactions at the interface between the electrolyte and the anode material. For example, the improved solvation structure allows for better Li^+ desolvation and more efficient charge transfer, even at low temperatures, which is particularly crucial for high-energy-density anode materials like Sb.[49] Moreover, these interactions help preserve the integrity of the SEI layer, enabling more efficient migration of Li^+, thus enhancing the cycling stability and rate performance of the battery. By maintaining a stable SEI layer despite the volume changes in alloy-based anodes, this approach contributes to preventing the degradation of the anode material and improving the overall battery life.[50,51]

In conclusion, optimizing solvent–solvent interactions within the electrolyte is a promising strategy to enhance the electrochemical performance of LIBs, especially for anode materials such as antimony. This optimization not only improves the battery's performance at low temperatures but also enhances the long-term stability of the electrode–electrolyte interface, thereby improving cycling performance and efficiency, ensuring a more stable and efficient battery system.

2.2. Li^+ transport at the electrolyte–electrode interface

Lithium dendrites are a significant factor in the degradation of lithium metal and graphite anodes, potentially causing internal short circuits and subsequent thermal runaway within batteries, thus significantly impacting their performance.[20,52] The formation of lithium dendrites is notably exacerbated in low-temperature environments. This phenomenon can be ascribed to the reduced migration rate of Li^+ ions as the temperature decreases, resulting in a relatively weaker electric field formed on the electrode surface.[53] An increase in overpotential is necessary to maintain sufficient electric field strength for facilitating Li^+ migration. However, an increase in overpotential brings about the formation of smaller and more numerous crystal nuclei on the electrode surface. This is because overpotential is inversely proportional to the size of the nuclei, and directly proportional to their number and density. Consequently, at low temperatures and low ion migration rates, numerous small-sized nuclei readily form and spatially cluster to create dendrites.[53] In low-temperature environments, the formation mechanism of the SEI is significantly affected. The decomposition rate of solvents in the electrolyte decreases, but due to the low potential of the anode, some incomplete reduction reactions still occur. These reactions generate byproducts, such as inorganic compounds (Li_2CO_3 and LiF) and organic compounds ($ROCO_2Li$), which gradually deposit on the electrode surface, forming a non-uniform and porous SEI layer.[54,55] At low temperatures, the decreased mobility of solvent molecules leads to slower SEI formation and results in a looser, more porous structure, increasing its non-uniformity. Since the ionic conductivity of the SEI is relatively low, an excessively thick SEI layer can significantly raise the impedance of the battery, thereby reducing its overall performance. Additionally, the slower desolvation process of Li^+ at low temperatures can cause more solvent molecules to be embedded in the SEI layer, leading to swelling and reduced stability. This instability further weakens the protective function of the SEI.[56] As lithium dendrites grow, the SEI layer on their surface regenerates and thickens continuously, which increases internal resistance and lowers coulombic efficiency. The combined effects of these phenomena further degrade the performance of lithium-ion batteries and elevate safety risks. The lithium dendrites at the electrode interface can be observed *via* low-temperature electron microscopy. The growth of these dendrites at the interface can also be assessed using low-temperature electron energy loss spectroscopy (Fig. 3a–c).[23,57] Maraschky *et al.*[61] propose that a reduction in the coefficient of Li^+ diffusion and a decrease in the maximal Li^+ migration concentration within the SEI both promote the development of lithium dendrites. Particularly under cold conditions, the continuous emergence of lithium dendrites at the electrode surface not only has the likelihood of penetrating the separator, giving rise to a short circuit in the LIBs, but can also persistently prompt SEI formation, which covers the dendrites. This results in a continuous increase in the thickness of the SEI, leading to a higher R_{SEI} and a lower coulombic efficiency.

Furthermore, desolvated Li^+ must diffuse through the SEI/cathode-electrolyte interface (CEI) film to interact with the electrode. Compared to Li^+ transport processes within the electrolyte, ion diffusion within the solid-state SEI/CEI film is significantly hindered at low temperatures. Therefore, enhancing the diffusion rate of ions within the SEI/CEI film is vital for improving the performance of LIBs in low-temperature environments. While research on the SEI film is well-established, studies on the CEI film are relatively scarce. The process of Li^+ intercalation into the anode at the electrolyte–electrode interface can be subdivided into two steps: (1) Li^+ transport through the SEI, and (2) charge transfer. At room temperature, the transit time of Li^+ through the SEI is generally considered to be between 10^{-5} and 10^{-3} s, while the charge transfer time ranges from 2 to 100 s.[58] At low temperatures, both R_{ct} and R_{SEI} increase as the temperature decreases (Fig. 3d). The SEI thickens at low temperatures, further reducing its ionic conductivity. This is because SEI formed from common organic electrolytes is non-uniform and highly porous, primarily composed of $ROCO_2Li$ and Li_2CO_3. These characteristics increase the impedance to interfacial Li^+ migration, leading to spatially uneven Li^+ flux, which further induces dendrite growth

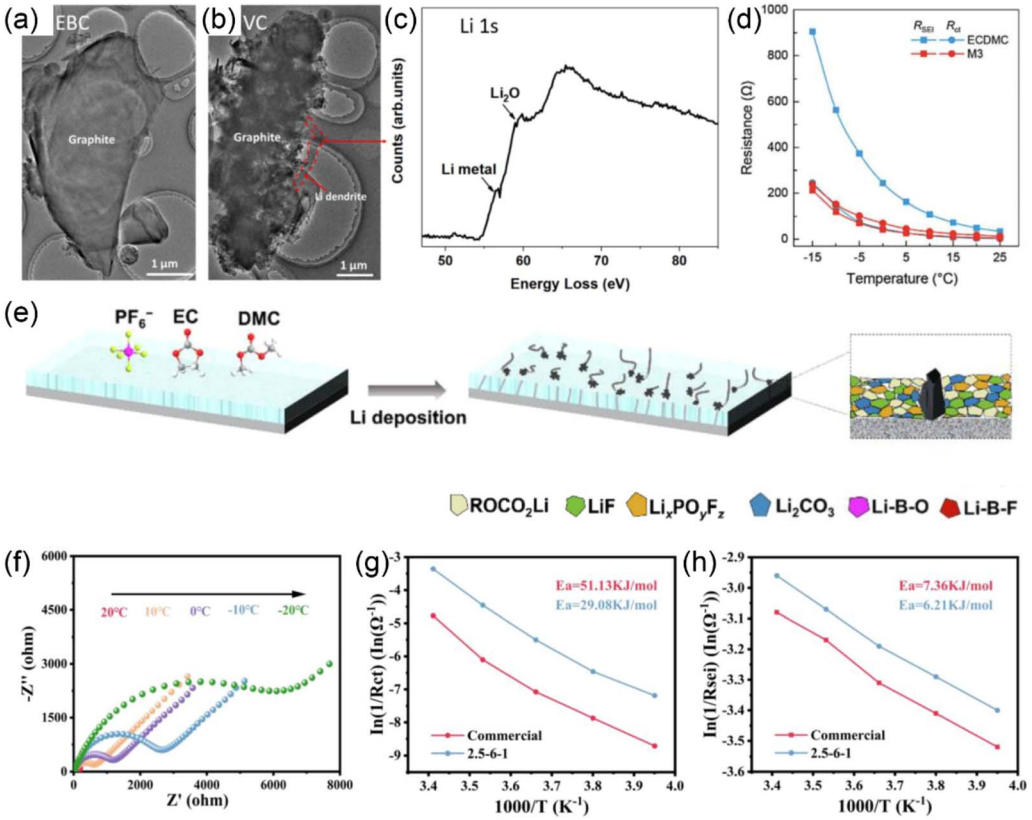

Fig. 3 (a and b) Low temperature transmission electron microscope (TEM) images of different systems of artificial graphite surface at low magnification. (c) Low temperature electron energy loss spectrum of Li 1s. Based on ref. 57. (d) Curve of R_{ct} and R_{SEI} of different electrolytes with temperature. Based on ref. 58. (e) Dendrite growth process in EC-based electrolyte. Based on ref. 59. (f) Impedance of EC-based electrolyte at different temperatures. (g and h) The activation energies of R_{ct} and R_{SEI}. Based on ref. 60.

(Fig. 3e).[59] In carbonate-based commercial electrolytes below 0 °C, R_{SEI} significantly becomes the limiting step in transport rates.[58] Zhang *et al.*[14] have shown that the temperature dependence of resistance is almost unaffected by the battery voltage, with R_{ct} increasing significantly as the temperature decreases. Below −20 °C, R_{ct} constitutes the majority of the total resistance in the battery, and the cyclic performance of LIBs is primarily limited by higher R_{ct}, mainly due to the slow kinetics of the battery reactions. The temperature dependence of R_{ct} is governed by the activation energy, following the thermally activated process described by the Arrhenius equation:[62]

$$1/R_{ct} = A_0 \exp(-E_a/RT)$$

where A_0 is a constant, E_a represents the activation energy, T is the temperature, and R is the gas constant. From the equation, it becomes apparent that the R_{ct} is determined by the temperature of the charge transfer process and its activation energy. A reduction in temperature combined with a rise in activation energy both lead to a higher R_{ct}. In particular, the impedance of EC-based commercial electrolytes increases significantly as the temperature decreases. Fitting the data to the Arrhenius equation clearly indicates that ion transport requires a high activation energy in both the charge transfer and SEI regions, which limits performance (Fig. 3f–h).[60] Thus, lowing the activation energy involved in the charge transfer process at low temperatures is the key to minimizing charge impedance. Nan *et al.*[63] developed an electrolyte based on LiFSI/EMC/TTE (molar ratio 2 : 3.3 : 3.3; LiFSI: lithium bis(fluorosulfonyl)imide; TTE: 1,1,2,2-tetrafluoroethyl-2,2,3,3-tetrafluoropropylether; EMC: ethyl methyl carbonate; denoted as DE), and the activation energies for the charge transfer and Li^+ transport processes through SEI were obtained by fitting. These were notably lower compared to those of the commercial electrolyte composed of $LiPF_6$/EC/DMC ($LiPF_6$: lithium hexafluorophosphate; DMC: dimethyl carbonate), indicating enhanced kinetics of the charge transfer and Li^+ transport process through SEI. This also shows that the impedance of Li^+ transport within SEI is reduced with the lowering of its activation energy.

In summary, slow ion transport kinetics is the primary factor limiting the performance of LIBs in low-temperature environments. The fundamental reason is the enhanced interactions between ions and solvents in the electrolyte under cold conditions, particularly the significant increase in solvent–solvent interactions. Given this situation, adjusting the electrolyte system to ameliorate this condition is entirely feasible. This includes tweaking the electrolyte components to achieve a more suitable balance between ion transport rates and lithium salt solubility at low temperatures. Other strategies such as

optimizing ion transport rates or controlling the fluidity of the electrolyte could also be explored to enhance low-temperature performance further.

2.3. Transport of Li^+ within electrode materials

Ion transport within electrode materials involves the intercalation and deintercalation of Li^+.[64] In the cathode, Li^+ intercalates from the electrolyte into the cathode material and deintercalates back into the electrolyte during the charging process. Conversely, in the anode, Li^+ intercalates from the electrolyte into the anode material and deintercalates back into the electrolyte during discharge. However, reductions in temperature significantly impair the diffusion capabilities of ions within the electrode materials.[65,66] Slow ion diffusion dynamics under low temperatures conditions can hinder the ions from reaching the active sites in the electrode materials, leading to a reduction in the capacity of LIBs.[67] Therefore, improving the transport kinetics of Li^+ within electrode materials is a critical issue that needs addressing, involving aspects at both the cathode and anode materials.

In terms of anode materials, graphite is one of the most commonly employed anode materials in LIBs under low-temperature conditions. At low temperatures, the transport speed of Li^+ within graphite layers is slow, leading to poor performance. Senyshyn *et al.*[18] found that changes in the thermodynamic stability of graphite anodes at low temperatures can lead to increased energy barriers, potentially obstructing Li^+ transport pathways and further limiting the performance of LIBs. Researchers have proposed various strategies to optimize the performance of graphite anodes. One common method involves regulating the graphite structure, such as by increasing interlayer distances to enhance Li^+ transport kinetics. Li *et al.*[68] proposed a slightly expanded spherical graphite as the host material, and achieved a good balance between high capacity and long-term cycle stability in lithium ion/metal storage by precisely regulating the degree of graphite sheet expansion. This adjustment was achieved through a chemical lithiation-

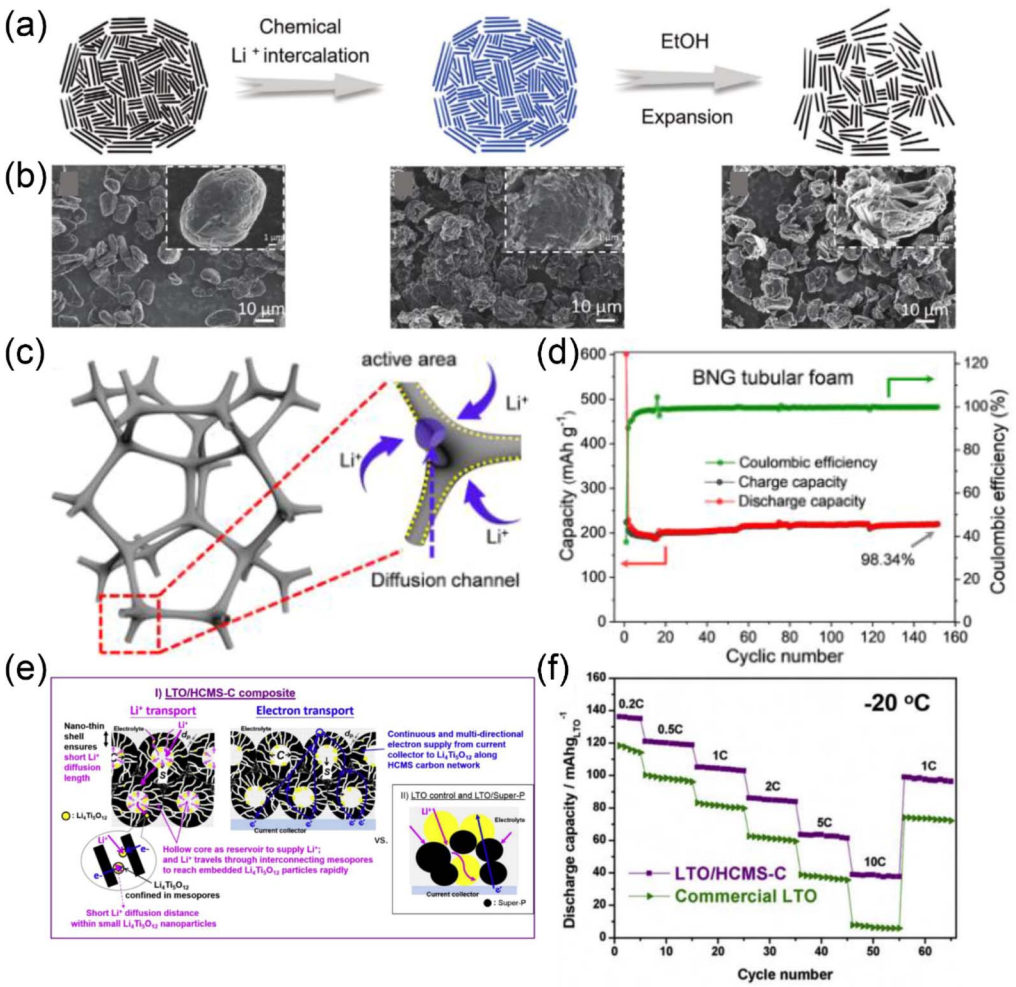

Fig. 4 (a) Diagram depicting the synthesis process of slightly expanded spherical graphite. (b) Scanning Electron Microscope (SEM) images of different degree of lithium. Based on ref. 68. (c) Branched nitrogen-doped graphite tubular foam anode and proposed lithium storage channel. (d) Performance during cycling of BNG tubular foam at −10 °C at 0.1C current density. Based on ref. 69. (e) Cross-section diagram of $Li_4Ti_5O_{12}$/HCMS carbon nanocomposite. (f) Multiplication performance of $Li_4Ti_5O_{12}$/HCMS carbon nanocomposites and commercial $Li_4Ti_5O_{12}$ at −20 °C. Based on ref. 70.

mild expansion process (Fig. 4a). After ethanol treatment, cracks appeared on the particle surface, and under H_2 gas pressure, the cracks in the layered structure further expanded. The degree of expansion was influenced by the gas flow rate and volume, with different lithium levels leading to varying degrees of expansion (Fig. 4b). The expanded graphite anode exhibited a specific capacity 1.5 times that of conventional graphite, with significantly increased capacity (96 mA h g^{-1}), even when cycled at 0.2C and −20 °C, and a capacity degradation of only 0.05% per cycle. Zhao *et al.*[71] used an oxidation modification method to increase the interlayer spacing of mesocarbon microbeads (MCMB), facilitating Li^+ transport kinetics. The modified MCMB electrode material still attained a specific capacity of 100 mA h g^{-1} at −40 °C, effectively improving its electrochemical performance under low temperatures. Dendritic tubular nitrogen-doped graphite anodes were fabricated using chemical vapor deposition (Fig. 4c). By introducing C–N functional groups with predominantly pyridine and pyrrole defects, the material formed curved knots and expanded plane branches. By introducing nitrogen atoms, the conductivity of the material was improved, along with an increase in the interlayer distances. This design significantly promoted Li^+ intercalation, deintercalation, and diffusion kinetics at low temperatures, thereby enhancing cyclic performance (Fig. 4d).[69] Moreover, the embedding of nanoscale tin can increase the distance between graphite layers, thereby improving the rate of Li^+ transport and enhancing the performance of the battery under low-temperature conditions.[72] Another method to overcome the drawbacks of graphite anodes is using alternative anode materials, for instance $Li_4Ti_5O_{12}$.[73] Compared to graphite, it has good reversibility of Li^+ intercalation/deintercalation, while accompanied by significant volume changes. Although the volume change might increase mechanical stress between the electrode material particles, negatively affecting the cyclic performance of LIBs, the structural stability and high reversibility of $Li_4Ti_5O_{12}$ help mitigate this impact. The high working voltage of 1.55 V means that during charging, the voltage of LIBs is unlikely to drop below the lithium plating potential, which reduces the likelihood of lithium dendrite formation and enhancing safety. However, $Li_4Ti_5O_{12}$ electrode materials have poor electronic conductivity and small Li^+ diffusion coefficients, which severely limit their electrochemical kinetics, especially at low temperatures.[74] Ho *et al.*[70] embedded $Li_4Ti_5O_{12}$ nanoparticles into a hierarchical macropore–mesoporous shell carbon network (HCMS carbon), producing $Li_4Ti_5O_{12}$/HCMS carbon nanocomposite materials (Fig. 4e). HCMS carbon is an ideal carrier for $Li_4Ti_5O_{12}$, which provides short and interconnected Li^+ diffusion paths between $Li_4Ti_5O_{12}$ particles and the Li^+ storage layer, as well as sufficient channels for continuous, multidirectional electron flow into $Li_4Ti_5O_{12}$ particles, achieving excellent low-temperature performance at high rates. At −20 °C, the composite material still exhibits a specific capacity of 42 mA h g^{-1} at 10C, which is 6.4 times that of commercial $Li_4Ti_5O_{12}$ (Fig. 4f). In summary, by regulating the graphite structure, embedding nanoparticles, and using alternative anode materials, the performance and stability of LIBs in low-temperature environments can be effectively improved. These strategies provide effective means to overcome the limitations of graphite anodes under low temperatures and offer significant insights into enhancing the performance and safety of LIBs in low-temperature conditions.

In low-temperature environments, cathode materials of LIBs also face a series of challenges, affecting the performance and stability of LIBs. To optimize electrochemical performance in cold temperatures, particularly improving the ionic/electronic conductivity and structural stability of cathode materials, various modifications are made to LIBs cathode materials. Surface coatings represent a viable approach to enhance the performance of the cathode material. Research shows that the introduction of small amounts of surface coatings can significantly enhance the conductivity of LIBs, reduce internal impedance, and mitigate side reactions at the electrode–electrolyte interface, thus efficiently improving the charge/discharge capacity and boosting the energy density of LIBs in low-temperature environments.[75,76] Chen *et al.*[77] used Ketjen Black (KB, EC-600JD) carbon as a carbon source to coat $Li_3V_2(PO_4)_3$ for the synthesis of a nanocomposite material. The KB carbon coating optimized the surface structure of the electrode and increased the contact area of the electrolyte with electrode, thereby promoting Li^+ transport rate. It also protected the material structure, achieving a discharge capacity of 92 mA h g^{-1} at a 4C rate at −30 °C. Additional innovative coating methods have been presented to further leverage the benefits of the carbon protective layer, such as using carbon nanotube-based coatings and forming bridging networks of graphene nanofibers.[78,79] Oxide coatings also help enhance the electrochemical performance of cathode materials under low-temperature conditions. For example, using Li_2O–B_2O_3 coatings on $LiNi_{1/3}Co_{1/3}Mn_{1/3}O_2$ significantly reduced R_{ct} and increased the discharge capacity from 37.2 to 101.9 mA h g^{-1} at −20 °C, with a capacity retention rate of 93.4% after 50 cycles.[80] Besides carbon and oxides, additional materials have been researched as coating options, such as conductive polymers and external element doping.[62,81] In summary, improvements to cathode materials and the application of coating technologies can effectively enhance the performance of LIBs at low temperatures.

3. Improving low-temperature performance of LIBs by adjusting electrolyte composition

The electrolyte, as a critical component of LIBs, plays an essential role in ionic conductivity, solvation structure, and the formation capabilities of the SEI/CEI, significantly impacting the transport characteristics of Li^+ between the anode and cathode. The limitations on Li^+ transport in the electrolyte at low temperatures are considerably greater than those within the electrode materials, indicating that modifying the electrolyte is crucial for improving the performance of LIBs in cold environments. The low-temperature performance of the electrolyte is

largely influenced by the viscosity and freezing point of the solvent, the extent of dissociation of the lithium salts, and the film-forming capability of additives. This section will discuss lithium salts, solvents, additives, and novel electrolyte systems from four perspectives.

3.1. Lithium salts

3.1.1. Optimizing single lithium salt. Lithium salts influence the performance of electrolytes under cold conditions by modifying the dissociation of anions and the formation capabilities of the SEI. Currently, $LiPF_6$ is extensively utilized as a commercial electrolyte lithium salt due to its ability to create a stable SEI on graphite anodes and its high ionic conductivity at room temperature. Nevertheless, when $LiPF_6$ is exposed to moisture, the resultant hydrofluoric acid corrodes the cathode active material, leading to capacity decay in LIBs.[82] Therefore, finding alternative lithium salts becomes a pathway to improving low-temperature performance.

Research indicates that some lithium salts, such as lithium hexafluoroarsenate ($LiAsF_6$), lithium tetrafluoroborate ($LiBF_4$), lithium bis(oxalate)borate (LiBOB), and lithium difluoro(oxalate)borate (LiDFOB), exhibit good ionic conductivity and film-forming capabilities at low temperatures and have the capability to replace $LiPF_6$. Shiao *et al.*[83] found that a 1 mol per L $LiAsF_6$-EC/EMC/MA/TOL (MA: methyl acetate; TOL: toluene) electrolyte had an ionic conductivity of 1.830 mS cm^{-1} at −40 °C and 1.100 mS cm^{-1} at −50 °C. Although $LiBF_4$ has a lower ionic conductivity compared to $LiPF_6$, it can provide a smaller R_{ct}, making $LiBF_4$ a high-quality lithium salt for low-temperature LIBs electrolytes.[84] However, the hydrolysis sensitivity, relatively low ionic conductivity, and suboptimal film-forming capability of $LiBF_4$ hinder its widespread application.[85] Similarly, despite LiBOB has good film-forming ability, its high viscosity and poor solubility in carbonate solvents limit its application in low-temperature LIBs.[86] In contrast, LiDFOB brings together the benefits of $LiBF_4$ and LiBOB. Its chemical structure consists of half-molecules of both salts, enabling the formation of highly stable SEI films on the anode and better solubility in linear carbonate solvents, resulting in lower solution viscosity and thereby optimizing LIBs for better performance in cold environments.[87] Yang *et al.*[88] dissolved 1 mol per L LiDFOB in PC/EC/EMC, and at −30 °C batteries using LiDFOB-based electrolyte retained 86% of their capacity at 20 °C with lower polarization. However, LiDFOB continuously forms SEI at low temperatures, resulting in higher interface impedance. Hence, the performance of pure LiDFOB-based electrolytes at low temperatures remains limited. LiFSI and lithium bis(trifluoromethanesulphonyl)imide (LiTFSI) have garnered considerable focus owing to their ideal thermal stability and lower R_{ct}.[26,88] Fan *et al.*[89] developed an ultra-low-temperature electrolyte comprised of 1.28 mol per L LiFSI-FEC/FEMC-D2 (FEC: fluoroethylene carbonate; FEMC: methyl (2,2,2-trifluoroethyl) carbonate; D2: tetrafluoro-1-(2,2,2-trifluoroethoxy) ethane), which provided a capacity of 96 mA h g^{-1} (56% of the capacity under room temperature conditions) at −85 °C in NCA||Li batteries. Additionally, Xu *et al.*[26] developed an electrolyte comprised of 0.75 mol per L LiTFSI-DIOX (DIOX: 1,3-dioxane) with a freezing point below −100 °C, maintaining 60% of room temperature capacity at a 0.1C rate at −80 °C. However, it is important to note that FSI^- and $TFSI^-$ anions can corrode the aluminum current collector of the cathode, worsening the performance of LIBs at both room temperature as well as in cold conditions.[82] In summary, optimizing the selection of lithium salts in the electrolyte can significantly improve the performance of LIBs in cold conditions, thereby promoting their broader application in cold climate conditions.

3.1.2. Mixed lithium salt strategy. Although various lithium salts are being studied as alternatives to $LiPF_6$, they each have their own shortcomings and have not displaced $LiPF_6$ in commercial applications. Thus, blending multiple lithium salts is viewed as a potential strategy to enhance the performance of LIBs at low temperatures (Fig. 5a).[90,96] To address the inadequate film-forming capability of $LiBF_4$, Lv *et al.*[91] dissolved a mixture of 0.3 mol per L $LiBF_4$ and 0.7 mol per L $LiPF_6$ in DMC/EMC/BA/EC (BA: butyl acrylate), which formed a porous and thin CEI on the cathode surface (Fig. 5b and c), facilitating Li^+ transport and thereby augmenting the performance of LIBs in low-temperature conditions. At −40 °C, this electrolyte still achieved a discharge capacity of 85 mA h g^{-1} during cycling. The $LiBF_4$–LiBOB (molar ratio 9 : 1) salt mixture developed by Zhang *et al.*[97] demonstrated superior performance in a PC/EC/EMC ternary solvent, enabling Li||$LiFePO_4$ batteries to achieve a discharge capacity of up to 100 mA h g^{-1} at 1C and −10 °C. Zhao *et al.*[98] explored the electrochemical behavior of different molar ratios of LiDFOB and $LiBF_4$ mixed salts. Results showed that the LiDFOB/$LiBF_4$ (molar ratio 1 : 1)-EC/DEC/DMS (DEC: diethyl carbonate; DMS: dimethyl sulfite) electrolyte system performed best at −40 °C, reaching a discharge capacity of 82.5 mA h g^{-1}, and maintaining 55.7% of the capacity recorded at room temperature and showing nearly 100% capacity retention after 50 cycles.

Concerning the issue of LiTFSI and LiFSI causing corrosion to the aluminum current collector of the cathode, Park *et al.*[92] proposed a solution using an electrolyte comprised of 0.8 mol per L LiFSI and 0.2 mol per L LiDFOB-EC/DEC, which effectively suppressed the corrosion of the aluminum current collector. The excellent inhibitory capability of LiDFOB in the LiFSI-based electrolyte against aluminum current collector corrosion is caused by the formation of a passivation layer composed of Al–F, Al_2O_3, and B–O (Fig. 5d). Additionally, the dual-salt electrolyte composed of LiTFSI and LiDFOB offered favorable ionic conductivity and outstanding electrochemical performance at low temperatures.[99] Lin *et al.*[93] developed a 2 mol per L LiTFSI/LiDFOB (molar ratio 4.3 : 1)-TMS/EA-10% FEC (TMS: sulfolane; EA: ethyl acetate) electrolyte, which provided good ionic conductivity at low temperatures (Fig. 5e) and maintained excellent electrochemical performance under conditions of charging to 4.6 V at a 1C current density at −40 °C (Fig. 5f). Yang *et al.*[100] prepared the electrolyte by dissolving 1.5 mol per L lithium triflate (LiOTF) and 0.2 mol per L $LiPF_6$ in a blend of diethylene glycol dimethyl ether (DEGDME) and 1,3-dioxolane (DOL) (volume ratio 1 : 1). This electrolyte exhibited low interface impedance and small charge transfer activation energy,

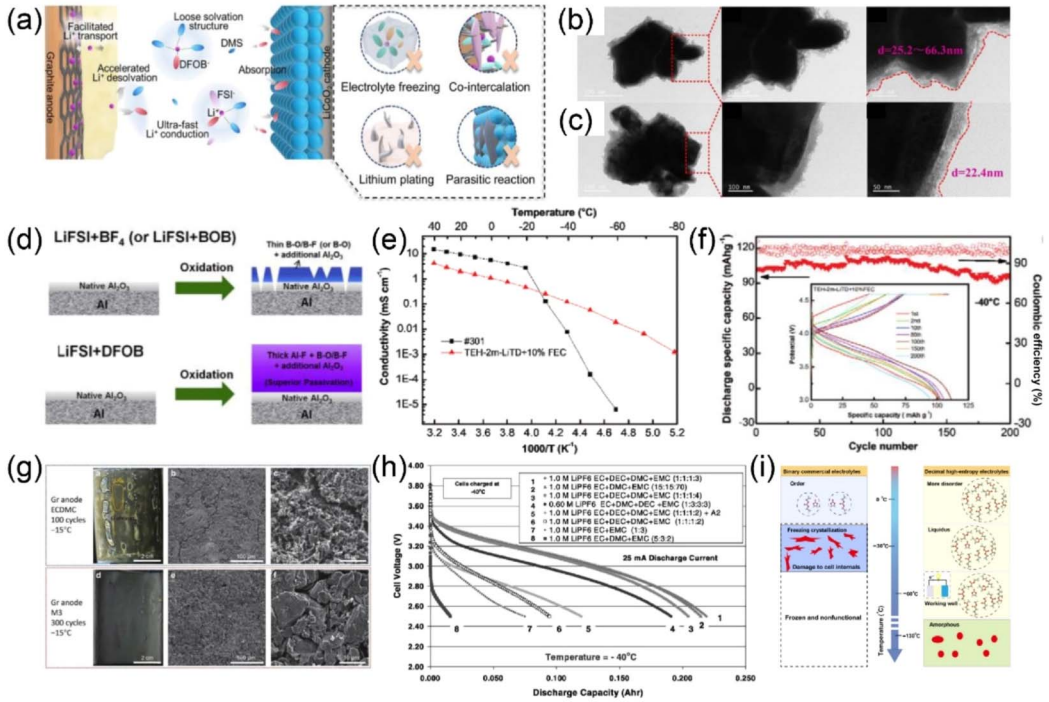

Fig. 5 (a) Advantages of mixed lithium salts in electrolytes. Based on ref. 90. (b and c) TEM analysis of various electrolytes following 50 cycles at −40 °C. Based on ref. 91. (d) Schematic diagram of forming passivation film on aluminum electrode using electrolytes of different lithium salts. Based on ref. 92. (e) Comparison of electrolyte conductivity at various temperatures. (f) Electrochemical performance of Li||NCM523 battery at −40 °C when charged to 4.6 V with current density of 1C. Based on ref. 93. (g) Optical and SEM images at the graphite anode at −15 °C. Based on ref. 58. (h) −40 °C, discharge capacity of batteries with different carbonate based electrolyte. Based on ref. 94. (i) Schematic diagram of the change of commercial binary and designed decimal high entropy electrolyte with temperature decreasing. Based on ref. 95.

allowing NCM||graphite full cells to maintain 58.3% compared to room temperature at −60 °C. Beyond binary lithium salts, Zhang *et al.*[101] developed a ternary lithium salt system of LiFSI/LiBOB/$LiPF_6$, which enhanced the rate performance and cycle stability of $LiFePO_4$ cathodes and graphite anodes. In summary, the mixed lithium salt strategy provides a novel solution to overcome the issues of performance degradation in traditional electrolytes at low temperatures and offers a new perspective for designing high-performance LIBs electrolytes.

3.2. Solvents

Carbonate solvents, such as EC and DMC, are commonly utilized in commercial electrolytes because of their high dielectric constants and good chemical stability. However, their relatively high melting points lead to significant increases in the viscosity of the electrolyte and rapid declines in conductivity under low-temperature conditions, which severely limits the low-temperature performance of LIBs.[102] Thus, using low-melting-point solvents in electrolytes is considered to be a strategy to enhance the low-temperature performance of LIBs. Additionally, adding suitable co-solvents to carbonate-based electrolytes to reduce the melting point and viscosity can also enhance the low-temperature performance of LIBs.

Carboxylate solvents exhibit lower viscosities and melting points in contrast to carbonate solvents, making them important alternative solvents to carbonates.[103] Due to its advantageous dielectric constant and low melting point of −87.5 °C, methyl propionate (MP) is a commonly used carboxylate. Holoubek *et al.*[104] selected MP as the primary solvent in the electrolyte and added FEC as an additive, enabling the battery to sustain optimal performance at temperatures as low as −65 °C and at a current density of 10C. Similarly, Cho *et al.*[105] proposed a 1 mol per L $LiPF_6$-MP/FEC (volume ratio 9 : 1) carboxylate-based electrolyte, which demonstrated significantly improved electrochemical cycling performance at −20 °C, greatly surpassing that of commercial standard carbonate-based electrolytes. Additionally, Yao *et al.*[58] studied an EC- and additive-free electrolyte composed of LiFSI/MA/FE/D3 (FE: fluorinated ether; D3: 1,1,2,2-tetrafluoroethyl 2,2,2-trifluoroethyl ether), which by anion decomposition provided a SEI as stable as those formed in EC-based systems, and the anion-derived SEI had better Li^+ transport properties at low temperatures. Due to improved interfacial transport performance, this electrolyte effectively suppressed lithium dendrite formation during low-temperature charging (Fig. 5g). Fluorinated carboxylate solvents are also considered good electrolyte solvents because fluorinated organic solvents have an extensive electrochemical stability window, non-flammability, and low melting points. Yang *et al.*[106] developed a novel fluorinated electrolyte composed of LiTFSI and ethyl trifluoroacetate (ETFA). Li^+–ETFA has very low binding energy and freezing point. The weaker binding energy between ETFA solvent and Li^+ promotes the desolvation process at low temperatures and

maintains a liquid state at extremely low temperatures, providing better electrochemical performance in LIBs than carbonate-based electrolytes at low temperatures.

Besides carboxylate solvents, early studies focused on adding co-solvents to EC-based electrolytes to reduce the melting point and viscosity, thereby enhancing LIBs' performance under low-temperature conditions. Smart *et al.*[107] reported a ternary mixed electrolyte containing 1 mol per L $LiPF_6$ in EC/DEC/DMC, which had an ionic conductivity of 1.0 mS cm^{-1} at −40 °C and produced a stable SEI. Then, adding varying quantities of EMC to EC/DEC/DMC further developed a quaternary all-carbonate high ionic conductivity electrolyte. Among these, the most promising electrolytes were 1.0 mol per L $LiPF_6$-EC/DEC/DMC/EMC (volume ratio 1 : 1 : 1 : 2) and 1.0 mol per L $LiPF_6$-EC/DEC/DMC/EMC (volume ratio 1 : 1 : 1 : 3).[94] At −40 °C, the electrolyte with a volume ratio of 1 : 1 : 1 : 3 exhibited superior performance in cold conditions (Fig. 5h), allowing the MCMB‖$LiNiCoO_2$ battery to achieve 65% of room temperature capacity. The benefits of this electrolyte were additionally confirmed in different battery systems. Liao *et al.*[65] studied the performance of the $LiFePO_4$/C cathode in 1.0 mol per L $LiPF_6$-EC/DEC/DMC/EMC (volume ratio 1 : 1 : 1 : 3) electrolyte, showing that Li‖$LiFePO_4$/C batteries maintained 84.8%, 66.9%, and 51.3% of room temperature capacity at 0 °C, −20 °C, and −40 °C, respectively.

Carboxylate solvents can also be added as co-solvents to carbonate-based electrolytes. Zhang *et al.*[108] incorporated methyl butyrate (MB) to the electrolyte, designing an electrolyte composed of 1 mol per L LiTFSI-DEC/EC/MB (volume ratio 1 : 1 : 1), resulting in a significant reduction in electrolyte and an increase in the ionic conductivity from 1.38 to 3.44 mS cm^{-1} at −20 °C. This electrolyte system formed a uniform SEI film on the anode, effectively suppressing the development of lithium dendrites. Similarly, the addition of ethyl acetate (EA) diminished the charge transfer activation energy in carbonate-based electrolyte (EC/DMC/EMC) from 48.36 to 33.01 kJ mol^{-1} at −20 °C, accelerating the charge transfer process and reducing the interfacial impedance at low temperatures.[109] Zhang *et al.*[95] blended various carbonate and carboxylate solvents, designing a novel high-entropy electrolyte 1 mol per L $LiPF_6$-EC/DEC/PC/EMC/EP/EA/MB/BA/MP/PB (EP: ethyl propionate; PB: propyl butyrate), which exhibited excellent ionic conductivity and capacity retention under ultra-low temperatures conditions down to −130 °C (Fig. 5i). This research provides new insights for designing LIBs electrolytes suitable for ultra-low temperature environments.

In addition to common carbonate and carboxylate solvents, new solvent components are being developed. Isoxazole (IZ) is a five-membered aromatic heterocyclic compound with a high boiling point, low melting point, and two electronegative heteroatoms (nitrogen and oxygen).[110] IZ, with its low viscosity and high dipole moment facilitate efficient Li^+ transport in IZ-based electrolytes, even at low temperatures. Tan *et al.*[13] observed that the ionic conductivity of IZ-based electrolytes was almost three times that of commercial electrolytes. However, IZ alone cannot form a stable SEI on the anode side to prevent co-intercalation of the solution. By adding LiDFOB and FEC additives, the IZ-based electrolyte achieved excellent long cycling performance, reaching a capacity of 187.5 mA h g^{-1} at −20 °C.

The types of common solvents in LIBs and their improvement strategies have been summarized, including a discussion on the performance of carboxylate solvents under low-temperature conditions, and ways to enhance the performance of electrolytes through the addition of different co-solvents. Additionally, the potential applications of novel solvents such as IZ and the research results on high-entropy electrolytes are introduced. These studies provide new ideas and directions for enhancing the performance of LIBs in cold conditions.

3.3. Additives

Due to the advantages of minimal dosage, rapid effectiveness, and low cost, the application of additives presents an effective and economical approach to enhance the low-temperature performance of LIBs and aid in the formation of a stable SEI (Fig. 6a).[111,115] Common additives include carbonates, sulfites, and lithium salts.

Among carbonate additives, vinylene carbonate (VC) stands out as one of the earliest to be commercially applied. During the discharge process, it is reduced to a radical anion, which facilitates the formation of a polymer that is beneficial for SEI formation. This further inhibits the solvent decomposition on the anode surface and enhances interfacial stability. Therefore, adding 1% VC to the electrolyte can significantly improve the first-cycle coulombic efficiency and cycle life of the battery.[116] FEC is also widely used commercially. Research has indicated that the addition of 2% FEC by volume can suppress the decomposition of part of the electrolyte solvent and form an excellent SEI layer on the electrode surface, reducing battery impedance and significantly enhancing the specific capacity and cycle stability of the battery.[115,117] Besides VC and FEC, Zhu *et al.*[118] introduced a mixed additive composed of 16% BA and 10% EC by volume, which facilitated the establishment of a steady SEI on the electrode surface. This also resulted in enhanced low-temperature ionic conductivity and discharge capacity, achieving a discharge capacity of 108.94 mA h g^{-1} at −40 °C. DMS, aside from being used as a solvent, can also serve as an additive in electrolytes. The reduction products of DMS have weak binding ability with Li^+, which facilitates the formation of a stable and uniform SEI with high ionic conductivity on the anode surface, thereby providing excellent low-temperature performance.[119] Additionally, propyl 4-methylbenzenesulfonate (PMBS), a new type of additive, has been developed (Fig. 6b). Adding PMBS to the electrolyte aids in forming a stable and low-impedance SEI and CEI, due to PMBS's propensity to decompose preferentially relative to solvent molecules. The LIBs containing 2% PMBS exhibited superior performance, with the capacity retention rate increasing from 55.37% to 98.02% after 100 cycles at −10 °C.[112] Qian *et al.*[57] designed and synthesized a novel carbonate molecule called erythritol bis(carbonate) (EBC), which merges two EC-like structures into a single molecule and exhibits

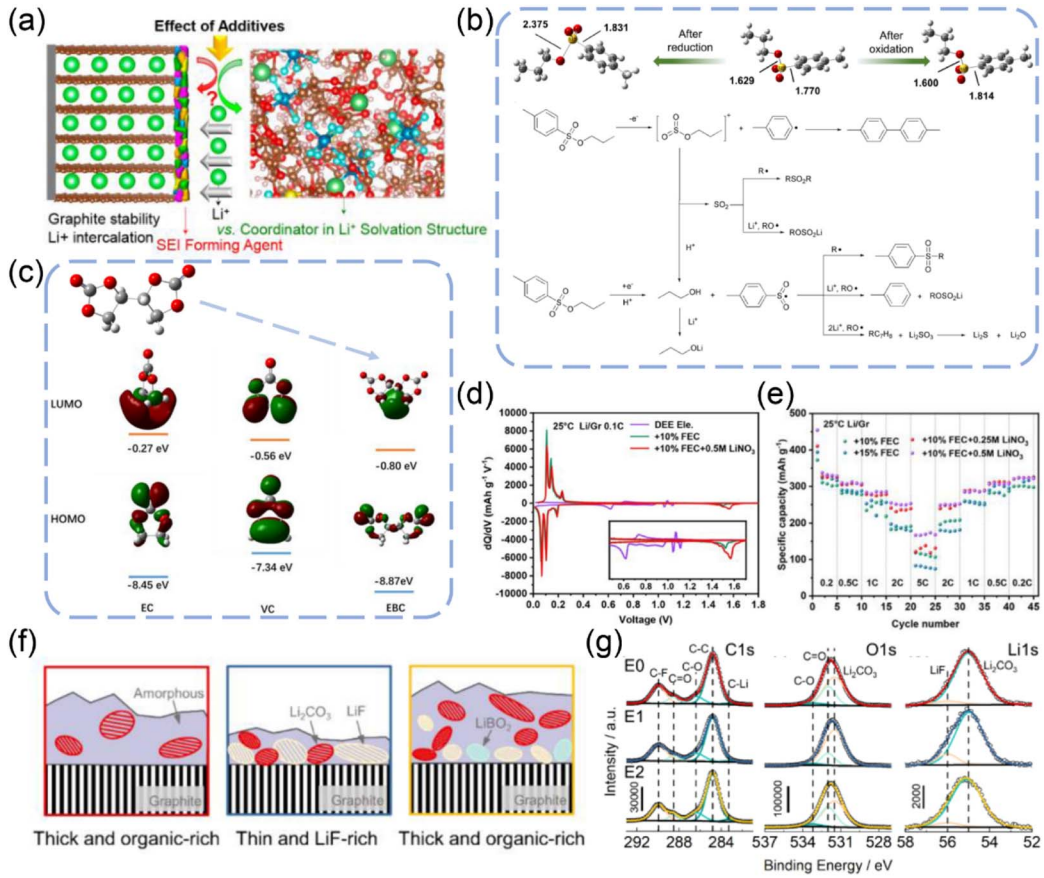

Fig. 6 (a) Illustration of the effect of additives on the graphite anode. Based on ref. 111. (b) PMBS bond length and potential mechanisms for formation on the electrode surface. Based on ref. 112. (c) The structure formula of EBC and the HOMO and LUMO levels of EC, EBC and VC. Based on ref. 57. (d) Cyclic Voltammetry curves of three electrolytes. (e) The rate performance of three electrolytes. Based on ref. 113. (f) Schematic illustration of SEIs formed on graphite in different electrolyte. (g) C 1s, O 1s, and Li 1s spectra of graphite electrodes after 3 cycles in different electrolyte. Based on ref. 114.

a lower LUMO energy level (Fig. 6c). A lower LUMO energy level for EBC compared to EC, indicating that it decomposes before EC is reduced. However, the weaker solvation of Li^+ by EBC does not involve a substantial chemical reaction with Li^+, which limits its reduction and thus forms a low-impedance and stable SEI.

Moreover, a small amount of lithium salt can also be used as an additive in electrolytes. Li *et al.*[120] proposed that adding lithium difluorophosphate ($LiPO_2F_2$) at a mass fraction of 2% to a 1 mol per L $LiPF_6$-DMC/EMC/PC/FEC electrolyte could enhance the electrochemical performance of LIBs under low-temperature conditions. $LiPO_2F_2$ addition encourages the development of a uniform, LiF-rich SEI layer on the electrode surface. This LiF-rich SEI possesses excellent ionic transport properties, facilitating the transport of Li^+ at low temperatures. Yang *et al.*[113] added lithium nitrate ($LiNO_3$) and FEC to an ether-based electrolyte. The addition of $LiNO_3$ further enhanced the reduction peak of FEC near 1.5 V (Fig. 6d), indicating the co-decomposition of FEC and $LiNO_3$. Moreover, the addition of FEC effectively addressed the issue of solvent co-intercalation in ether-based electrolytes. The combined addition of FEC and $LiNO_3$ not only preserved the preferential decomposition characteristic of FEC, but also introduced LiN_xO_y with high ionic conductivity into the SEI, aiding the rapid transport kinetics of Li^+, and enhancing the electrochemical performance of LIBs (Fig. 6e). Additionally, $LiBF_4$ can serve not only as a substitute salt for $LiPF_6$, but also as a supplement salt. Qin *et al.*[114] studied the addition of 0 M, 0.05 M and 0.1 M $LiBF_4$ into a 1 M $LiPF_6$-EC/EMC/MB (2 : 2 : 6 by volume) electrolyte, labeled as E0, E1 and E2, respectively. The results showed that the addition of trace amounts of $LiBF_4$ enhances the coordination between PF_6^- and Li^+, weakens the interaction between EC and Li^+, and forms a dense, LiF-rich SEI. The electrolyte containing $LiBF_4$ exhibited a higher capacity, indicating that more anions were reduced and a large amount of SEI was accumulated. In the E0 electrolyte, the decomposition of PF_6^- was limited, and the graphite edge mainly grew in amorphous regions scattered with a few crystalline particles. In contrast, in the E1 electrolyte, a continuous film formed on the graphite surface, primarily composed of LiF and $LiBO_2$, with LiF being the dominant component. However, in the E2 electrolyte, which had a higher concentration of $LiBF_4$, the inorganic components in the SEI were mainly $LiBO_2$, which could not form an effective protective film, leading to poor passivation performance (Fig. 6f). The SEI

formed in the E1 electrolyte, as identified through XPS analysis, contained the highest proportion of inorganic substances, including higher contents of Li_2CO_3 and LiF, further verifying its high interfacial stability and dynamic advantages (Fig. 6g).

This suggests that by regulating the solvation structure of $LiBF_4$, an appropriate amount of $LiBF_4$ plays a role in forming a highly protective, LiF-rich SEI, thereby enhancing LIB performance. Similarly, LiDFOB can also be used as a supplement salt for $LiPF_6$. As an additive, LiDFOB preferentially decomposes on the surface of the lithium anode and high nickel cathode. $DFOB^-$ preferentially reduces and oxidizes, forming a strong, boron-rich interfacial film with high electronic insulation, which effectively inhibits the consumption of active lithium and the decomposition of the electrolyte. On the cathode surface, key CEI components such as BF_3, BF_2OH and BF_2OBF_2 form strong coordination bonds with lattice oxygen, inhibiting the loss of lattice oxygen and slowing down the irreversible structural degradation process. On the lithium anode, the SEI, rich in $BF_2CH_2CH_2COOLi$ and $BF_2OCH_2CH_2$-$CH_2CH_2OBF_2$, generated by LiDFOB decomposition, has low adhesion, reduces the energy barrier for lithium deposition/stripping, promotes uniform lithium deposition, and inhibits the formation of lithium dendrites.[121] Through continuous research and innovation, electrolyte additives are poised to provide crucial support and assurance for the performance improvement and application expansion of future LIBs.

3.4. Constructing a novel electrolyte system

3.4.1. Local high concentration electrolyte. High concentration electrolytes (HCE) and localized high concentration electrolyte (LHCE) systems have garnered considerable research interest in recent years. HCEs are highly appreciated for their oxidative stability, thermal stability, ability to form quality SEI, and unique solvation structures. In the solvation structure of HCE, lithium salts exist in various forms within the lithium salt-solvent complexes, such as solvent-separated ion pairs (SSIP), contact ion pairs (CIPs), and aggregates (AGGs).[122] However, HCEs encounter obstacles at low temperatures, including high viscosity, reduced wettability, and poor ionic transport,

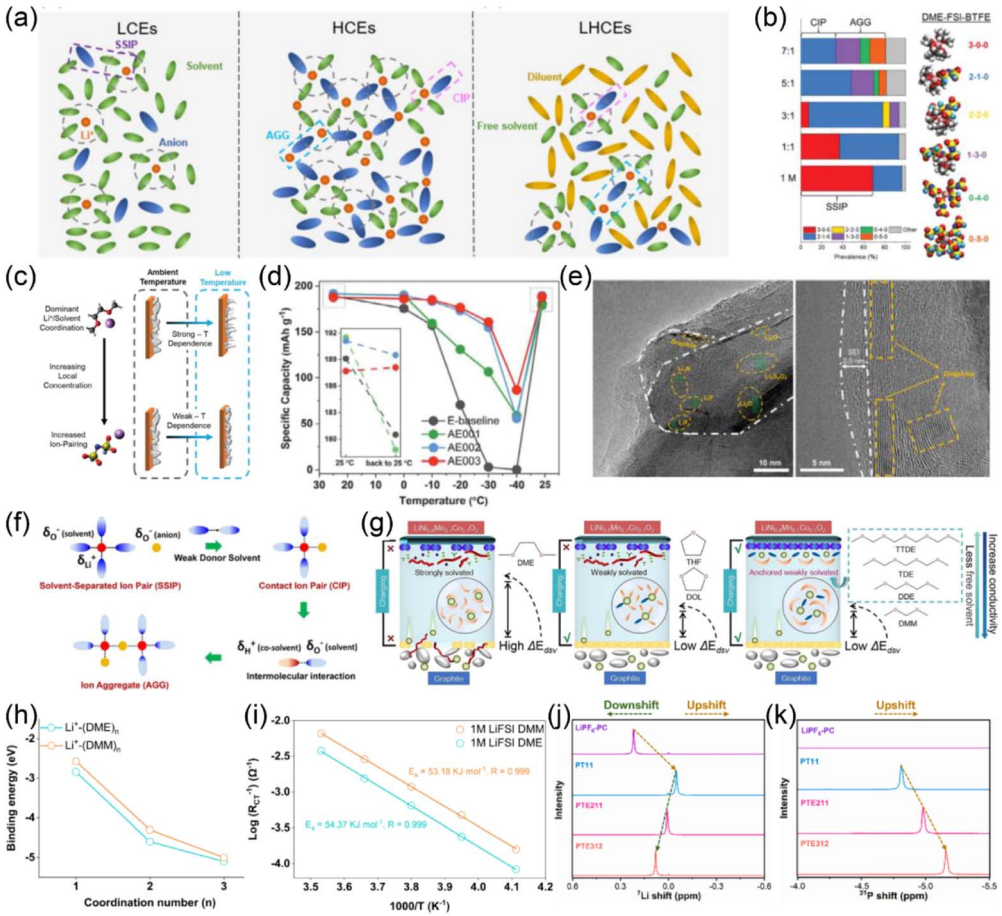

Fig. 7 (a) Solvation structure of electrolytes with low concentration, high concentration and local high concentration. Based on ref. 123. (b) Distribution analysis of various solvation structures and representative MD snapshots. (c) Design concept of solvation at room temperature and low temperature. Based on ref. 124. (d) Low temperature performance at 0.2C discharge rate. Based on ref. 125. (e) TEM images of graphite negative electrodes. Based on ref. 126. (f) Formation of special solvated structures in weakly solvated electrolytes. Based on ref. 127. (g) Mechanism of solvation structure of polyoxymethylene ether electrolyte. Based on ref. 128. (h) Diagram of Li^+ binding energy of solvation of DME and DMM as a function of coordination number. (i) Desolubilization and activation energy of two electrolytes. Based on ref. 129. (j and k) NMR spectra of different electrolytes. Based on ref. 2.

restricting the application of HCE-based electrolyte systems in LIBs at low temperatures. Researchers have proposed a new approach involving the addition of inert solvents to HCEs, forming LHCEs (Fig. 7a).[123,130] The inert diluent, while not dissolving the lithium salt, is miscible with the solvent, thus reducing the concentration of lithium salts without affecting the original Li^+ solvation structure in HCEs.

Holoubek *et al.*[124] proposed an LHCE based on LiFSI/dimethoxyethane (DME) with bis(2,2,2-trifluoroethyl) ether (BTFE) as the diluent. By modifying the molar ratio between lithium salt and solvent, an ionic pairing transition occurs when the local concentration of lithium salts exceeds 4 mol L^{-1}. This transition alters the balance between the inner and outer layers of the solvation structure, resulting in the formation of an HCE rich in AGGs (Fig. 7b). This altered structure facilitates the formation of a fluoride-rich SEI, thus promoting uniform Li deposition in $Li/LiNi_{0.8}Co_{0.1}Mn_{0.1}O_2$ (NCM811) batteries at low temperatures (Fig. 7c). Regulating the solvation structures of ionic pairs positively impacts the reversibility of Li metal under low-temperature conditions. Zhang *et al.*[125] proposed three types of LHCEs: 1.4 mol per L LiFSI-DMC/TTE (molar ratio 2.2 : 3), 1.4 mol per L LiFSI-DMC/VC/TTE (molar ratio 2 : 0.2 : 3), and 1.4 mol per L LiFSI-DMC/EC/TTE (molar ratio 2 : 0.2 : 3), designated as AE001, AE002, and AE003, respectively. Compared to conventional carbonate-based electrolytes, these three LHCEs significantly enhance battery performance over an extensive temperature range. The LHCE containing a small amount of EC showed superior low-temperature performance, achieving a discharge capacity of 160.7 mA h g^{-1} at −30 °C and a 0.2C rate (Fig. 7d), possibly due to the ability of EC to establish a thinner and more robust SEI. Additionally, a new short-chain fluorinated diluent known as 1,1,2,2-tetrafluoroethyl methyl ether (TFME) has been developed. An LHCE was prepared by adding TFME to a MA-based electrolyte, enabling LIBs to maintain high performance in low-temperature environments, delivering 80.85% of their room temperature discharge capacity at 0.2C and −50 °C.[131] Jiang *et al.*[126] used BTFE as the diluent in a 1.5 mol per L LiFSI and DME-based electrolyte for the production of an LHCE. This LHCE was able to form a predominantly inorganic, uniform, and robust SEI (Fig. 7e), effectively inhibiting the co-intercalation of ether solvents into the graphite anode. The graphite||Li cells exhibited superior electrochemical performance, delivering a discharge capacity of 90 mA h g^{-1} at 0.1C at −20 °C. Under room temperature conditions, the cells achieved 220 mA h g^{-1} at 4C, demonstrating high-rate capabilities. The LHCE demonstrated excellent cycling stability, maintaining approximately 85.5% of its initial capacity after 200 cycles at 4C. 1,2-bis(1,1,2, 2-tetrafluoroethoxy)ethane (BTFEE), as a diluent with weak solvation ability, has been used in the study of electrolyte systems.[132] Due to its weak solvation ability with salts, BTFEE is primarily used as a diluent, though it can also partially participate in the dissolution process, thereby influencing the makeup of the electrode–electrolyte interfaces, particularly the formation of inorganic compounds rich in Li_2O and LiF. Unlike traditional non-coordination diluents, BTFEE can form weak coordination with Li^+ in LHCE and participate in the first solvation sheath structure. By optimizing the ratio of DME, which has strong solvation ability, to BTFEE, which has weak solvation ability, an inorganic-rich SEI and CEI can be effectively customized, significantly improving the cycle stability of the battery. In terms of electrochemical performance, lithium metal batteries with a NCM811 cathode, with a loading of 4 mA h cm^{-2}, retained 80% of their initial capacity after 470 cycles when cycled in the voltage range of 2.8–4.4 V.[132] Lai *et al.*[133] designed a locally high-concentration electrolyte based on tetrahydrofuran (THF), selecting THF as the alkaline solvent due to its low viscosity (0.53 cP), low melting point (−108 °C), and high solubility for LiTFSI. This electrolyte exhibits lower viscosity and higher conductivity at low temperatures compared to traditional high-concentration electrolytes, which helps improve the Li^+ diffusion at low temperatures. In addition to high oxidation stability, the higher anion ratio in the solvated structure further facilitates the charge transfer process.

To further enhance the performance of the battery at low temperatures, researchers introduced 1,1,2,2-tetrafluoroethyl-2,2,3,3-tetrafluoro-propylether (HFE) as a diluent to create LHCE from HCE. The addition of HFE not only diminishes the viscosity of HCE by destroying the 3D network structure, but also preserves the unique solvation structure of HCE due to the HFE's weak coordination ability with Li^+. This LHCE system effectively combines the high ion mobility characteristic of low-concentration electrolytes with the unique solvation properties of high-concentration electrolytes. Furthermore, this electrolyte demonstrates superior low-temperature performance, delivering over 70% capacity at −70 °C and maintaining 72.5 mA h g^{-1} (≈77.1%) capacity for 200 cycles at a 1C rate at −40 °C. Even when the rate increases to 5C, the battery still operates well at −40 °C. This work shows that solvation regulation significantly influences the kinetics of cells at low temperatures and offers a design method for future electrolyte development. In summary, the formation of LHCEs by adding inert solvents is a successful strategy to optimize the performance of HCEs in cold conditions. These studies provide valuable insights for extending LIBs' applications to extreme environments.

3.4.2. Weak solvent electrolyte. In traditional electrolytes, the strong binding capacity of Li^+ with solvents prevents anions from coordinating more extensively with Li^+, hindering the formation of an anion-derived SEI. At low temperatures, the fluidity of the electrolyte decreases, leading to a decline in ionic conductivity and a slowdown in chemical reaction rates on the electrode surfaces. This further exacerbates the degradation of the SEI and contributes to the decline in LIBs performance. Using weakly solvating electrolytes composed of solvents with weak solvation binding energy is an effective approach. Due to their special solvation structures, these electrolytes commonly feature CIPs and AGGs, which promote the formation of an inorganically-rich SEI at the electrode surface (Fig. 7f).[127] This SEI is more stable and conductive, especially at low temperatures. Cao *et al.*[134] designed a weakly solvating electrolyte in which the fluorinated solvent could form weaker interactions, such as hydrogen bonds and van der Waals forces, and also interacted less intensively with Li^+, thereby reducing the

solvation capacity of Li^+ to address the desolvation challenges. This electrolyte, composed of 1 mol per L LiFSI, FEC, bis(2,2,2-trifluoroethyl) carbonate (BTFC), and weakly solvating ETFA with a fluorinated structure, further weakens the solvation capacity of the electrolyte while effectively lessening its viscosity and melting point. Full cells using this electrolyte attained a high specific capacity of 103.5 mA h g^{-1} at −20 °C and showed stable performance over 100 cycles. By changing the ion–dipole interaction in the Li^+ solvent sheath, FEC, BTFC solvent molecules and FSI^- anions preferentially decompose to form an SEI rich in LiF and other inorganics, which effectively prevents the continuous reduction of organic solvents and the structural damage of electrodes. Liu *et al.*[128] systematically designed a class of weakly solvated polyoxymethylene ether electrolyte for LIBs by controlling the length of the –O–CH_2–O– fragment. The –O–CH_2–O– fragment in the solvent is capable of forming a weak four-membered ring Li^+ coordination structure, and an increased number of fragments can anchor the solvent to Li^+ without significantly sacrificing ionic dissociation ability (Fig. 7g).

Cyclic voltammetry confirms that the designed molecules can achieve reversible solvent-free co-intercalation of Li^+ into a graphite cathode at conventional concentrations. Due to the enhanced "anchoring effect" and the increased chain length, the oxidation stability of the electrolyte is improved. Among them, dipolyformaldehyde dimethyl ether (DDE) showed both high oxidation stability and excellent electrode reaction kinetics. Additionally, the weak solvation ability of DDE enables anions to participate in the solvation structure, facilitating the formation of an inorganic-rich CEI/SEI interface on the electrode surface. In terms of electrochemical performance, Gr‖NCM811 Ah-class pouch cells with the DDE-based electrolyte retained 70.85% capacity after 1000 cycles at room temperature and 75.86% capacity after 400 cycles at −20 °C, demonstrating excellent cycle stability and low-temperature performance. Yang *et al.*[135] designed a 1 mol per L LiTFSI-ETFA/FEC (volume ratio 7 : 3) weakly solvating electrolyte, which demonstrated excellent low-temperature performance by maintained 78% of room temperature capacity at −30 °C in a graphite‖$LiFePO_4$ battery. Ma *et al.*[129] compared two ether solvents, dimethoxymethane (DMM) and DME. As shown in Fig. 7h, regardless of coordination number, the interaction of DMM with Li^+ is weaker than that of DME. Compared to DME-based electrolytes, the solvation sheath of the electrolyte with DMM containes fewer and weaker coordinating solvents, thus DMM-based electrolytes exhibit faster desolvation kinetics (Fig. 7i). Rapid desolvation in weakly solvating electrolytes achieves smoother lithium deposition and higher coulombic efficiency, significantly enhancing the safety of battery operation under low-temperature conditions. Moreover, Li‖SPAN full cell shows a high initial discharge capacity at −40 °C (422.3 mA h g^{-1}) and excellent capacity retention (63.8% after 120 cycles), indicating that the weakly solvating electrolyte effectively supports stable and efficient performance even under extreme conditions. Liu *et al.*[136] developed a weakly solvated electrolyte system with IZ as the main solvent, consisting of 1.0 M LiFSI dissolved in IZ, fluorobenzene (FB) as a non-coordinating solvent, and FEC as a film-forming additive. Through the dipole–dipole interaction between FB and IZ, this system effectively reduces the desolvation energy of Li^+. Its weak solvation ability allows more anions to enter the solvation sheath, promoting the formation of CIPs and AGGs, thereby enhancing the Li^+ transport rate and maintaining high ionic conductivity across a wide temperature range. At −20 °C, this electrolyte system achieves a reversible capacity of 200.9 mA h g^{-1} in a graphite half-cell, nearly three times that of traditional EC-based electrolytes. Chen *et al.*[2] designed a novel weakly solvating electrolyte with a "drag effect" by introducing bis(2,2,2-trifluoroethyl) ethyl phosphonate (TFEP) and EMC into a $LiPF_6$–PC-based electrolyte. TFEP, with a higher degree of fluorination, has weaker Li^+ coordinating capabilities, which allows PF_6^- to co-squeeze into the first solvation sheath layer of Li^+, forming an anion-induced ion–solvent coordination structure (AI-ISC). Alternatively, TFEP acts as a flame-retardant solvent, significantly reducing the electrolyte's flammability. However, the interaction of Li^+ with TFEP is too weak to break the coordination bonds of Li^+–PC and Li^+–PF_6^-, making it challenging for Li^+ to break free from the solvation complex. Thus, a third solvent, EMC, which exhibits a stronger affinity for Li^+ and a comparable coordination capability to TFEP, is incorporated into the aforementioned PC–TEFP. This addition effectively facilitates Li^+ transport without disrupting the AI-SIC structure, thereby reducing the strength of interactions between Li^+–PC and Li^+–PF_6^-. The "drag effect" markedly lowers the binding energy between Li^+–PC and Li^+–PF_6^-, as demonstrated by nuclear magnetic resonance characterization (Fig. 7j and k). Due to its low Li^+ desolvation energy, elevated Li^+ transference number, and strong electrochemical compatibility of the AI-ISC structure, the weakly solvating electrolyte endows the graphite anode with outstanding cycle stability (100% capacity retention after 400 cycles), superb low-temperature performance (approximately 79% and 62.5% capacity retention at −40 °C and −50 °C, respectively), and safety features (verified through overcharge, squeeze, thermal shock, and nail penetration tests).[2]

Overall, employing weakly solvating electrolytes is an effective strategy to overcome the low-temperature performance limitations of traditional electrolytes in LIBs. This research direction will continue to advance battery technology, providing more stable and reliable energy solutions for next-generation electric vehicles and portable electronic devices.

3.4.3. Liquefied gas electrolyte. In addition to the aforementioned electrolyte systems, recent research on liquefied gas electrolytes with low melting points and enhanced safety has garnered significant attention for their potential to improve the performance of LIBs. Among these, electrolytes based on fluoromethane (FM) are particularly noted for their low melting points and low viscosity. However, the low lithium salt solubility and high polarization of FM limit its practical application. Researchers have introduced THF as a co-solvent to address this issue, successfully enhancing the solubility of lithium salts and forming a uniform SEI rich in LiF (Fig. 8a), thereby achieving excellent low-temperature performance.[137] Nevertheless, the operational temperature range and oxidative stability of this

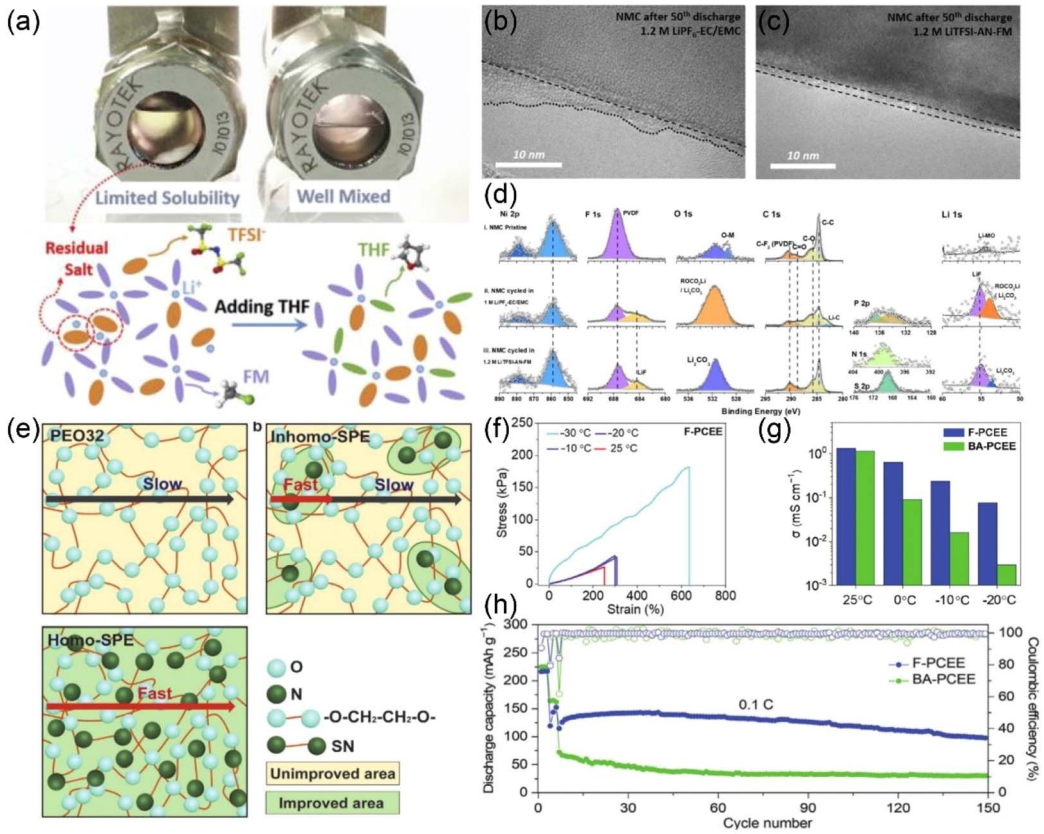

Fig. 8 (a) Solubility test and solvation mechanism diagram of liquefied gas electrolyte. Based on ref. 137. (b and c) Cyclic performance of two electrolytes at low temperature at 0.1C. (d) XPS map of two electrolytes interfacial membranes. Based on ref. 138. (e) Schematic diagram of Li^+ transport mode for PEO based electrolytes. Based on ref. 139. (f) Stress–strain curves of F-PCEE at 25 °C, −10 °C, −20 °C and −30 °C. (g) Conductivity of two electrolytes at different temperatures. (h) Cycle performance of the battery at −10 °C and 0.1C. Based on ref. 140.

electrolyte still require further improvement. Yang *et al.*[138] discovered that using acetonitrile (AN) as a co-solvent with FM in the preparation of liquefied gas electrolytes resulted in higher lithium salt solubility (1.2 mol per L LiTFSI) and a noticeably wider temperature range (−60 °C ~55 °C). In these liquefied gas electrolytes, a uniformly thick and more extensively covering CEI was formed on the surface of NMC cathode materials (Fig. 8b and c). The XPS analysis revealed that the CEI formed in carbonate-based electrolytes exhibits organic compound characteristics, consisting of decomposition products from the carbonate-based electrolytes (Fig. 8d). On the contrary, the CEI formed in liquefied gas electrolytes includes LiF, S–O, and N–O species derived from the decomposition of LiTFSI and FM, facilitating the formation of a protective interfacial phase, which further enhances battery performance. Under the conditions of 3 mA cm^{-2} and 3 mA h cm^{-2}, the average coulombic efficiency for lithium metal cycling over 200 cycles reached 99.4%.[138] Researchers have tested the safety of batteries using liquefied gas electrolytes through nail penetration tests. Traditional LIBs undergo internal short circuits at the moment of nail penetration, leading to a rapid local temperature increase and thus thermal runaway. Batteries using liquefied gas electrolytes rapidly vaporize the internal electrolyte upon nail penetration, causing a swift drop in battery temperature, followed by a gradual return to room temperature. The rapid vaporization of the electrolyte obstructs the internal ionic pathways, thereby preventing internal short circuits caused by nail penetration.[141] Subsequently, liquefied gas electrolytes based on difluoromethane (DFM) were also proposed.[141] Compared to FM-based electrolytes, DFM-based liquefied gas electrolytes exhibit lower pressure, lower flammability, and a wider operational temperature range, opening new directions and possibilities for research on liquefied gas electrolytes. Yin *et al.*[142] developed a new liquefied gas electrolyte based on dimethyl ether (Me_2O) and PC, aimed at improving the electrochemical performance of batteries under extreme temperature conditions. The electrolyte maintains high ionic conductivity (>3.5 mS cm^{-1}) over a wide temperature range from −70 °C to 60 °C. Me_2O, with its low desolvation energy, enhances the performance of the electrolyte at both high rates and low temperatures. Additionally, because the C–O–C bond in Me_2O has higher Lewis basicity than the C–F bond, its ability to dissolve salts is superior to other gaseous solvents, such as FM and DFM, while its excellent compatibility with lithium metal makes it suitable for applications across a wide temperature range. To further optimize the performance of the electrolyte, the researchers replaced DME in the traditional $LiBF_4$–DME–PC formulation with Me_2O. By optimizing the ratio of Me_2O to PC,

the electrolyte's transmission and discharge performance was significantly improved. Due to the weak affinity between Me_2O and Li^+, anions take a more dominant role in the solvation structure, enhancing the electrolyte's desolvation process and improving its rate performance and low-temperature operability. Thanks to its rapid desolvation and transport dynamics, the optimized electrolyte achieves high utilization of CF_x, exhibits exceptional rate performance at room temperature and −60 °C, and demonstrates exceptional energy output within the extended temperature window of −70 °C to 55 °C. In Li/CF_x cells using a 4.3 mg cm^{-2} loading CF_x cathode, the cell delivered 780 mA h g^{-1} (91% room-temperature capacity retention) under a 10 mA g^{-1} discharge current at −60 °C. Furthermore, when 50 mg cm^{-2} CF_x was utilized, the cell still displayed 706 mA h g^{-1} (84% room-temperature capacity retention) at −60 °C, and the average discharge voltage remained above 2.1 V.[142]

In summary, as a novel type of electrolyte system, liquefied gas electrolytes offer good low-temperature performance and enhanced safety, providing new insights and solutions for the development of lithium-ion batteries. However, further research and improvements are still needed to meet the demands of practical applications.

3.4.4. Polymer electrolyte. Compared to traditional liquid electrolytes, polymer electrolytes exhibit superior interfacial stability and enhanced safety, making them excellent candidate electrolytes for LIBs. Xiang *et al.*[143] presented a novel polymerized 1,3-dioxolane (PDE) electrolyte, formulated with a multifunctional tris(pentafluorophenyl)borane (TB) additive. The addition of TB led to the formation of a PDE that exhibited excellent flame resistance, substantially extended operational temperature range, and boosted oxidative stability. This polymer electrolyte also possesses the capability to form a highly stable and LiF-rich SEI film, high ionic conductivity, and reduced interfacial impedance. It demonstrated exceptional performance in low-temperature conditions in Li–S batteries, maintaining a capacity of about 700 mA h g^{-1} at −20 °C, with the capacity recoverable after 24 hours of rest at low temperatures.[143] Succinonitrile (SN) was introduced into a poly(ethylene oxide) (PEO)-based electrolyte, forming a uniform solid-state polymer electrolyte (Homo-SPE).[139] By varying the molar ratio of SN and PEO to 1 : 4, rapid Li^+ transport channels were formed within the Homo-SPE (Fig. 8e), resulting in a hundredfold increase in ionic conductivity, rendering it applicable in mid to low-temperature environments. Compared to the original PEO-based electrolyte, the NMR ^{7}Li spectrum of Homo-SPE shifted forward by 0.50 ppm, with the peak moving to a higher field indicating weakened interactions of PEO–Li^+. Therefore, the addition of SN could mitigate the affinity between PEO and Li^+, further explaining the mechanism of rapid Li^+ transport in

Table 1 New electrolyte system and electrochemical performance

Electrolyte system	Electrolyte	Cell system	Capacity (LT)	Capacity (25 °C)	Ref.
High-concentration	3 mol per L $LiPF_6$/EA/FEC (9 : 1 by vol.)	Graphite‖NCM811	0.85 A h (−40 °C, 0.1C)	0.9 A h (300 cycles, 2C)	21
	5 mol per L LiTFSI/THF	Li‖LMO	50.1 mA h g^{-1} (−40 °C, 0.1C)	300 cycles, 84.1% (1C)	133
	LiFSI/DME (1 : 1.4 by mol)	Li‖NCM333	—	500 cycles, 92% (1C)	145
Local high-concentration	3.3 mol per L LiFSI/AN/TTE (1 : 1 by vol.)	Graphite‖NCM111	110 mA h g^{-1} (−30 °C, 0.1C)	250 cycles, 94% (0.5C)	146
	1.4 mol per L LiFSI/DMC/TTE (2.2 : 3 by mol)	Graphite‖NCM811	106.5 mA h g^{-1} (−30 °C, 0.2C)	400 cycles, 100% (1/3C)	125
	1.4 mol per L LiFSI/DMC/VC/TTE (2 : 0.2 : 3 by mol)	Graphite‖NCM811	154.9 mA h g^{-1} (−30 °C, 0.2C)	400 cycles, 98.6% (1/3C)	125
	1.4 mol per L LiFSI/DMC/EC/TTE (2 : 0.2 : 3 by mol)	Graphite‖NCM811	160.7 mA h g^{-1} (−30 °C, 0.2C)	600 cycles, 94.2% (1/3C)	125
	1.5 mol per L LiFSI/DME/BTFE (1 : 2 by vol.)	Graphite‖Li	90 mA h g^{-1} (−20 °C, 0.1C)	200 cycles, 85.5% (4C)	126
	2 mol per L $LiPF_6$ + 0.04 mol per L LiDFOB/DMC/HFE (1 : 1 by vol.)	Graphite‖Li	240 mA h g^{-1} (−20 °C, 0.1C)	210 mA h g^{-1} (2C)	147
Weak solvation	1 mol per L LiTFSI/ETFA/FEC (7 : 3 by vol.)	Graphite‖Li	183 mA h g^{-1} (−30 °C, 0.05C)	200 cycles, 84.5% (5C)	135
	1 mol per L LiFSI/DMM	Li‖LTO	100 cycles, 75.9% (−20 °C, 0.2C)	200 cycles, 77.3% (0.5C)	129
	1 mol per L $LiPF_6$/VC ethyl fluoroacetate (3 : 97 by vol.)	Graphite‖$LiCoO_2$	2.87 A h (−40 °C, 0.1C)	400 cycles, 87.7% (1C)	148
Liquefied gas	1.2 mol per L LiTFSI + 1 mol per L AN in FM	Li‖NCM622	89 mA h g^{-1} (−60 °C, 1/15C)	500 cycles, 96.5% (1/3C)	138
	0.3 mol per L LiFSI + 0.35 mol per L DME in DFM	Li‖NCM622	108 mA h g^{-1} (−20 °C, 0.05C)	151 mA h g^{-1} (0.05C)	141
Polymer	2 mol per L LiTFSI/DOL + 3 wt% TB	Li–S	700 mA h g^{-1} (−20 °C, 0.5C)	550 cycles, 62.3% (0.2C)	143
	1 g PEO + 0.203 g LiTFSI + 0.45 g SN	Li‖$LiFPO_4$	141.5 mA h g^{-1} (0 °C, 0.03C)	750 cycles, 93.3% (0.5C)	139

Homo-SPE. This electrolyte exhibited good cyclic performance and high capacity retention (97.3%).[139] Park *et al.*[140] developed a fluorine-containing plastic-crystal embedded elastic electrolyte (F-PCEE) for the stable operation of solid lithium metal batteries at −10 °C. F-PCEE has a bicontinuous structure, consisting of an SN-based plastic crystal phase embedded in a 2,2,3,4,4,4-hexafluorobutyl acrylate (HFBA) based elastomer matrix. The electrolyte exhibits excellent performance at −10 °C, with Li^+ conductivity reaching up to 0.23 mS cm^{-1}, and enhanced elastic properties with a fracture strain of about 300% (Fig. 8f and g), effectively overcoming the tradeoff between ionic conductivity and mechanical properties. Additionally, F-PCEE facilitates the formation of a LiF-rich SEI on lithium metal surfaces, enabling full cells with lithium metal anodes and NCM811 cathodes to achieve excellent cycling performance at −10 °C. After 150 cycles at 0.1C, the battery's capacity retention rate reaches 85.3%, with a cutoff voltage of up to 4.5 V (Fig. 8h), representing one of the best cycling performances among solid polymer electrolyte-based lithium metal batteries at −10 °C, particularly for nickel-rich cathode systems. In contrast, poly(-butyl acrylate)-based PCEE (BA-PCEE) exhibits lower ion conductivity and mechanical properties at −10 °C, leading to rapid capacity decay in full cells.[140] Motivated by the high-efficiency water purification and soil stabilization properties of aquatic plants, Liu *et al.*[144] prepared poly(1,3-dioxolane) (PDOL) through *in situ* ring-opening polymerization of DOL. This process created a 3D desolvation area, which improved Li^+ desolvation at the interface. This resulted in the production of an amorphous gel polymer electrolyte with high Li^+ ionic conductivity (5.73 mS cm^{-1}). A greater number of anions contribute to the solvation structure, culminating in the formation of a stable SEI derived from anions, which enhances Li^+ transport through the SEI.[144] Despite the many advantages of polymer electrolytes, such as lightweight, ultra-thin, and flexibility, they still face some challenges at low temperatures. Compared to liquid electrolytes, polymer electrolytes generally have poorer ionic conductivity and performance at low temperatures. Therefore, although polymer electrolytes hold potential, further research and improvements are needed to enable their widespread application in cold environments (Table 1).

4. Conclusions

Over the past few decades, the performance decline of LIBs in low-temperature environments has been a focal point of concern. To address this challenge, scientists have invested considerable efforts in the development of electrolytes suitable for low temperatures, dedicating substantial resources to this pursuit. This paper provides a comprehensive review of the causes for the performance decline of LIBs in low-temperature environments and highlights the latest research progress in aspects ranging from lithium salts, solvents, additives to novel electrolyte systems.

Firstly, by improving the formula of the electrolyte, reducing its melting point and viscosity, effectively preventing the solidification of the electrolyte at low temperature, and accelerating the transmission rate of Li^+. Secondly, the formation of an inorganically-rich SEI at the electrolyte–electrode interface effectively reduces interfacial impedance, thereby facilitating Li^+ transport at the interface and enhancing the low-temperature performance of the battery. Moreover, innovative designs in electrode material structures also contribute to enhancing the performance of LIBs in cold conditions.

Despite significant progress in accelerating Li^+ transport and constructing stable electrolyte–electrode interfaces, several challenges remain under low-temperature conditions. Firstly, the desolvation of Li^+ at low temperatures is a critical performance limitation, necessitating further research into Li^+ solvation structures with low desolvation energy. Secondly, while an SEI rich in LiF and with low impedance is crucial for low-temperature LIBs, its formation mechanism and the Li^+ migration mechanism still require in-depth investigation. Thirdly, the role of electrode materials in low-temperature LIBs is also critical. It is necessary to ensure rapid Li^+ transport within the electrode materials, considering the compatibility between the electrolyte and electrode materials.

In future research, characterization techniques and theoretical studies will play an increasingly important role. Novel *in situ* characterization techniques, such as *in situ* Raman spectroscopy, electrochemical SEM and TEM, can monitor reactions and structural changes inside the battery in real time, providing more data to support an in-depth understanding of the behavior mechanism of the electrolyte. At the same time, computational methods such as molecular dynamics simulations and density functional theory will play a key role in the prediction and design of new low-temperature electrolytes. By combining these experimental and theoretical approaches, scientists are expected to develop more systematic and effective design strategies, laying the foundation for the future development of more efficient, stable and economical low-temperature electrolytes. Overall, the development of low-temperature electrolytes is not only crucial for improving the application of LIBs in extreme environments, but it will also have a broad impact on the fields of electric vehicles, aerospace, and energy storage. Through continuous technological innovation and in-depth theoretical exploration, future lithium-ion batteries will be able to maintain excellent performance across a wider temperature range, further promoting the commercialization of low-temperature electrolytes.

Data availability

No primary research results, software or code have been included and no new data were generated or analysed as part of this review.

Author contributions

Changlin Liu: conceptualization, writing – original draft. Lizhi Sheng: writing – review & editing, funding acquisition. Lili Jiang: project administration, review & editing.

Conflicts of interest

There are no conflicts to declare.

Acknowledgements

The authors acknowledge financial support from the Department of Science and Technology of Jilin Province (20240304104SF, 20240304103SF), Research and Innovation Fund of Beihua University for the Graduate Students (Major Project 2023012). Lizhi Sheng is grateful to the China Scholarship Council for the financial support (No. 202108220125).

References

1 C. P. Grey and D. S. Hall, Prospects for lithium-ion batteries and beyond—a 2030 vision, *Nat. Commun.*, 2020, **11**, 1.
2 L. Chen, J. Wang, M. Chen, Z. Pan, Y. Ding, Z. Song, X. Ai, Y. Cao and Z. Chen, "Dragging effect" induced fast desolvation kinetics and −50 °C workable high-safe lithium batteries, *Energy Storage Mater.*, 2024, **65**, 103098.
3 C. Qiu, L. Jiang, Y. Gao and L. Sheng, Effects of oxygen-containing functional groups on carbon materials in supercapacitors: A review, *Mater. Des.*, 2023, **230**, 111952.
4 X. Lin, L. Sheng, J. Yang, Y. Zhang, H. Shi, Y. Li, K. Wu, M. Han, X. Zhou and L. Jiang, Flexible films with three-dimensional ion transport channels: Carbon nanotubes@MnO_2 as interlayer spacers in porous graphene electrodes for high-performance supercapacitors, *J. Alloys Compd.*, 2024, **990**, 174455.
5 Z. Deng, Y. Jia, Y. Deng, C. Xu, X. Zhang, Q. He, J. Peng, H. Wu and W. Cai, Coordination structure regulation in non-flammable electrolyte enabling high voltage lithium electrochemistry, *J. Energy Chem.*, 2024, **96**, 282–290.
6 L. Jiang, H. Shi, M. Han, Y. Zhang, J. Liang, J. Chen, S. Geng, L. Tong and L. Sheng, Rearrangement of pore structure-enabled micropore-dominant N,O Co-doped carbon for ultrafast charge/discharge rate supercapacitors at commercial-scale mass loading, *ACS Sustainable Chem. Eng.*, 2024, **12**, 18422–18433.
7 J. Wang, Q. Zheng, M. Fang, S. Ko, Y. Yamada and A. Yamada, Concentrated electrolytes widen the operating temperature range of lithium-ion batteries, *Adv. Sci.*, 2021, **8**, 2101646.
8 Y. Li, G. Zheng, G. Liu, Z. Yuan, X. Huang and Y. Li, A review on electrode and electrolyte for lithium ion batteries under low temperature, *Electroanal*, 2023, **35**, e202300042.
9 Y. Wang, L. Ren, Q. Zhang, A. H. Pato, J. Liu, X. Lu and W. Liu, Fluorine-rich electrolyte additive for achieving dendrite-free lithium anodes at low temperatures, *ACS Appl. Mater. Interfaces*, 2024, **16**, 47674–47682.
10 J. Hao, W. Liu, Y. Tian, J. Wu, H. Guo, G. Zhang, Y. Yi, C. Han, F. Kang and B. Li, Unraveling the mechanism of methyl acetate additive for reinforcing the solid electrolyte interface on graphite anodes, *J. Mater. Chem. A*, 2024, **12**, 22679–22688.
11 X. Chen, Z. Li, H. Zhao, J. Li, W. Li, C. Han, Y. Zhang, L. Lu, J. Li and X. Qiu, Dominant solvent-separated ion pairs in electrolytes enable superhigh conductivity for fast-charging and low-temperature lithium ion batteries, *ACS Nano*, 2024, **18**, 8350–8359.
12 S. Lei, Z. Zeng, H. Yan, M. Qin, M. Liu, Y. Wu, H. Zhang, S. Cheng and J. Xie, Nonpolar cosolvent driving LUMO energy evolution of methyl acetate electrolyte to afford lithium-ion batteries operating at −60 °C, *Adv. Funct. Mater.*, 2023, **33**, 2301028.
13 S. Tan, U. N. D. Rodrigo, Z. Shadike, B. Lucht, K. Xu, C. Wang, X.-Q. Yang and E. Hu, Novel low-temperature electrolyte using isoxazole as the main solvent for lithium-ion batteries, *ACS Appl. Mater. Interfaces*, 2021, **13**, 24995–25001.
14 S. S. Zhang, K. Xu and T. R. Jow, Electrochemical impedance study on the low temperature of Li-ion batteries, *Electrochim. Acta*, 2004, **49**, 1057–1061.
15 T. R. Jow, S. A. Delp, J. L. Allen, J.-P. Jones and M. C. Smart, Factors limiting Li^+ charge transfer kinetics in Li-ion batteries, *J. Electrochem. Soc.*, 2018, **165**, A361.
16 Y. Mo, G. Liu, Y. Yin, M. Tao, J. Chen, Y. Peng, Y. Wang, Y. Yang, C. Wang, X. Dong and Y. Xia, Fluorinated solvent molecule tuning enables fast-charging and low-temperature lithium-ion batteries, *Adv. Energy Mater.*, 2023, **13**, 2301285.
17 Y. Deng, S. Feng, Z. Deng, Y. Jia, X. Zhang, C. Xu, S. Miao, M. Yao, K. Wu, Y. Zhang and W. Cai, Rationalizing Na-ion solvation structure by weakening carbonate solvent coordination ability for high-voltage sodium metal batteries, *J. Energy Chem.*, 2023, **87**, 105–113.
18 A. Senyshyn, M. J. Mühlbauer, O. Dolotko and H. Ehrenberg, Low-temperature performance of Li-ion batteries: The behavior of lithiated graphite, *J. Power Sources*, 2015, **282**, 235–240.
19 C. Hogrefe, T. Waldmann, M. Hölzle and M. Wohlfahrt-Mehrens, Direct observation of internal short circuits by lithium dendrites in cross-sectional lithium-ion *in situ* full cells, *J. Power Sources*, 2023, **556**, 232391.
20 G. Zhang, X. Wei, G. Han, H. Dai, J. Zhu, X. Wang, X. Tang and J. Ye, Lithium plating on the anode for lithium-ion batteries during long-term low temperature cycling, *J. Power Sources*, 2021, **484**, 229312.
21 Z. Li, N. Yao, L. Yu, Y.-X. Yao, C.-B. Jin, Y. Yang, Y. Xiao, X.-Y. Yue, W.-L. Cai, L. Xu, P. Wu, C. Yan and Q. Zhang, Inhibiting gas generation to achieve ultralong-lifespan lithium-ion batteries at low temperatures, *Matter*, 2023, **6**, 2274–2292.
22 Z. He, Y. Chen, F. Huang, Y. Jie, X. Li, R. Cao and S. Jiao, Fluorinated solvents for lithium metal batteries, *Acta Phys.–Chim. Sin.*, 2022, **38**, 2205005.
23 Y. Li, Y. Li, A. Pei, K. Yan, Y. Sun, C.-L. Wu, L.-M. Joubert, R. Chin, A. L. Koh, Y. Yu, J. Perrino, B. Butz, S. Chu and Y. Cui, Atomic structure of sensitive battery materials and interfaces revealed by cryo–electron microscopy, *Science*, 2017, **358**, 506–510.

24 S. Yuan, S. Cao, X. Chen, J. Wei, Z. Lv, H. Xia, J. Li, H. Zhang, L. Liu, C. Tian, L. Chen, W. Zhang, Z. Xing, H. Li, S. Li, Q. Zhu, X. Feng and X. Chen, Deshielding anions enable solvation chemistry control of $LiPF_6$-based electrolyte toward low-temperature lithium-ion batteries, *Adv. Mater.*, 2024, **36**, e2311327.

25 N. Yao, X. Chen, Z.-H. Fu and Q. Zhang, Applying Classical, *Ab Initio*, and machine-learning molecular dynamics simulations to the liquid electrolyte for rechargeable batteries, *Chem. Rev.*, 2022, **122**, 10970–11021.

26 J. Xu, X. Wang, N. Yuan, J. Ding, S. Qin, J. M. Razal, X. Wang, S. Ge and Y. Gogotsi, Extending the low temperature operational limit of Li-ion battery to −80 °C, *Energy Storage Mater.*, 2019, **23**, 383–389.

27 Y. Zou, Y. Shen, Y. Wu, H. Xue, Y. Guo, G. Liu, L. Wang and J. Ming, A designed durable electrolyte for high-voltage lithium-ion batteries and mechanism analysis, *Chem.–Eur. J.*, 2020, **26**, 7930–7936.

28 Z. Xie, J. He, Z. Xia, Q. Cai, Z. Tang, J. Cai, Y. Chen, X. Li, Y. Fan, L. Xing, Y. Shen and W. Li, Synergistic interphase modification with dual electrolyte additives to boost cycle stability of high nickel cathode for all-climate battery, *J. Energy Chem.*, 2023, **86**, 197–207.

29 M. Rakhatkyzy, A. Belgibayeva, G. Kalimuldina, A. Nurpeissova and Z. Bakenov, Enhancing low-temperature characteristics of graphite anode by comprehensive modification of electrolyte, *Electrochem. Commun.*, 2023, **157**, 107606.

30 A. J. Ringsby, K. D. Fong, J. Self, H. K. Bergstrom, B. D. McCloskey and K. A. Persson, Transport phenomena in low temperature lithium-ion battery electrolytes, *J. Electrochem. Soc.*, 2021, **168**, 080501.

31 K. Xu, Nonaqueous liquid electrolytes for lithium-based rechargeable batteries, *Chem. Rev.*, 2004, **104**, 4303–4418.

32 Y. Chen, Q. He, Y. Zhao, W. Zhou, P. Xiao, P. Gao, N. Tavajohi, J. Tu, B. Li, X. He, L. Xing, X. Fan and J. Liu, Breaking solvation dominance of ethylene carbonate *via* molecular charge engineering enables lower temperature battery, *Nat. Commun.*, 2023, **14**, 8326.

33 P. Lai, Y. Zhang, B. Huang, X. Deng, H. Hua, Q. Chen, S. Zhao, J. Dai, P. Zhang and J. Zhao, Revealing the evolution of solvation structure in low-temperature electrolytes for lithium batteries, *Energy Storage Mater.*, 2024, **67**, 103314.

34 S. Lei, Z. Zeng, M. Liu, M. Qin, Y. Wu, Y. Zhu, S. Cheng and J. Xie, Nonflammable cosolvent enables methyl acetate-based electrolyte for 4.6 V-class lithium-ion batteries operating at −60 °C, *Chem. Eng. J.*, 2023, **478**, 147180.

35 A. Boudenne, R. Tlili and Y. Candau, Thermophysical and thermal expansion properties, *Wiley Encyclopedia of Composites*, 2011, pp. 1–22.

36 N. Yao, X. Chen, X. Shen, R. Zhang, Z. H. Fu, X. X. Ma, X. Q. Zhang, B. Q. Li and Q. Zhang, An atomic insight into the chemical origin and variation of the dielectric constant in liquid electrolytes, *Angew. Chem., Int. Ed.*, 2021, **133**, 21643–21648.

37 B. Pal, S. Yang, S. Ramesh, V. Thangadurai and R. Jose, Electrolyte selection for supercapacitive devices: a critical review, *Nanoscale Adv.*, 2019, **1**, 3807–3835.

38 J. Hou, M. Yang, D. Wang and J. Zhang, Fundamentals and challenges of lithium ion batteries at temperatures between −40 and 60 °C, *Adv. Energy Mater.*, 2020, **10**, 1904152.

39 H. Hu, J. Li, Q. Zhang, G. Ding, J. Liu, Y. Dong, K. Zhao, M. Yu, H. Wang and F. Cheng, Non-concentrated electrolyte with weak anion coordination enables low Li-ion desolvation energy for low-temperature lithium batteries, *Chem. Eng. J.*, 2023, **457**, 141273.

40 X. Chen, X. Q. Zhang, H. R. Li and Q. Zhang, Cation–solvent, cation–anion, and solvent–solvent interactions with electrolyte solvation in lithium batteries, *Batteries Supercaps*, 2019, **2**, 128–131.

41 X. Chen and Q. Zhang, Atomic insights into the fundamental interactions in lithium battery electrolytes, *Acc. Chem. Res.*, 2020, **53**, 1992–2002.

42 H. Xie, H. Liang, P. Kumar, H. Cheng, F. Zhao, Y. Wang, T. Cai, W. Wahyudi, Z. Ma, Q. Li and J. Ming, Intermolecular interaction mediated potassium ion intercalation chemistry in ether-based electrolyte for potassium-ion batteries, *Adv. Funct. Mater.*, 2024, **34**, 2401118.

43 T. Cai, Y. Wang, F. Zhao, Z. Ma, P. Kumar, H. Xie, C. Sun, J. Wang, Q. Li, Y. Guo and J. Ming, Graphic, quantitation, visualization, standardization, digitization, and intelligence of electrolyte and electrolyte-electrode interface, *Adv. Energy Mater.*, 2024, **14**, 2400569.

44 H. Liang, P. Kumar, Z. Ma, F. Zhao, H. Cheng, H. Xie, Z. Cao, L. Cavallo, Q. Li and J. Ming, Electrolyte intermolecular interaction mediated nonflammable potassium-ion sulfur batteries, *ACS Energy Lett.*, 2024, **9**, 3536–3546.

45 Q. Li, G. Liu, P. Kumar, F. Zhao, Y. Wang, T. Cai, Y. Chen, H. Xie, W. Wahyudi, Z. Ma and J. Ming, Ultralow concentration nonflammable electrolytes mediated by intermolecular interactions for safer potassium-ion sulfur batteries, *Adv. Funct. Mater.*, 2024, 2416714.

46 H. Xie, H. Cheng, P. Kumar, Y. Wang, H. Liang, T. Cai, F. Zhao, Z. Cao, L. Cavallo, Z. Ma, Q. Li and J. Ming, Thermodynamic and kinetic behaviors of electrolytes mediated by intermolecular interactions enabling high-performance lithium-ion batteries, *ACS Nano*, 2024, **18**, 22503–22517.

47 Q. Sun, Z. Cao, Z. Ma, J. Zhang, W. Wahyudi, G. Liu, H. Cheng, T. Cai, E. Xie, L. Cavallo, Q. Li and J. Ming, Interfacial and interphasial chemistry of electrolyte components to invoke high-performance antimony anodes and non-flammable lithium-ion batteries, *Adv. Funct. Mater.*, 2023, **33**, 2210292.

48 Q. Sun, Z. Cao, Z. Ma, J. Zhang, H. Cheng, X. Guo, G.-T. Park, Q. Li, E. Xie, L. Cavallo, Y.-K. Sun and J. Ming, Dipole–dipole interaction induced electrolyte interfacial model to stabilize antimony anode for high-safety lithium-ion batteries, *ACS Energy Lett.*, 2022, **7**, 3545–3556.

49 Y. Zou, G. Liu, Y. Wang, Q. Li, Z. Ma, D. Yin, Y. Liang, Z. Cao, L. Cavallo, H. Kim, L. Wang, H. N. Alshareef, Y. K. Sun and J. Ming, Intermolecular interactions mediated nonflammable electrolyte for high-voltage lithium metal batteries in wide temperature, *Adv. Energy Mater.*, 2023, **13**, 2300443.

50 A. Huang, Z. Ma, P. Kumar, H. Liang, T. Cai, F. Zhao, Z. Cao, L. Cavallo, Q. Li and J. Ming, Low-temperature and fast-charging lithium metal batteries enabled by solvent-solvent interaction mediated electrolyte, *Nano Lett.*, 2024, **24**, 7499–7507.

51 T. Cai, W. Wahyudi, P. Kumar, Z. Ma, Q. Sun, H. Xie, Y. Wang, F. Zhao, Z. Cao, L. Cavallo, Q. Li and J. Ming, Overlooked challenges of interfacial chemistry upon developing high energy density silicon anodes for lithium-ion batteries, *Mater. Sci. Eng. R Rep.*, 2024, **161**, 100854.

52 J. Liu, X. Li, D. Wu, H. Wang, J. Huang and J. Ma, Anion-acceptor electrolyte additive strategy for optimizing electrolyte solvation characteristics and electrode electrolyte interphases for Li||NCM811 battery, *Acta Phys.–Chim. Sin.*, 2024, **40**, 2306039.

53 K. Yan, J. Wang, S. Zhao, D. Zhou, B. Sun, Y. Cui and G. Wang, Temperature-dependent nucleation and growth of dendrite-free lithium metal anodes, *Angew. Chem., Int. Ed.*, 2019, **131**, 11486–11490.

54 S. Yoon, K. Cavallaro, B. Park, H. Yook, J. Han and M. McDowell, Controlling solvation and solid-electrolyte interphase formation to enhance lithium interfacial kinetics at low temperatures, *Adv. Funct. Mater.*, 2023, **33**, 2302778.

55 R. Chen, S. Miao, Y. Jia, X. Zhang, J. Peng, K. Zhang, F. Wu, J. Zhao, Z. Li and W. Cai, A review of detecting Li plating on graphite anodes based on electrochemical methods, *J. Mater. Chem. A*, 2024, **12**, 33427–33447.

56 C. Xu, P. Jing, Z. Deng, Q. Liu, Y. Jia, X. Zhang, Y. Deng, Y. Zhang and W. Cai, Rectifying solid electrolyte interphase structure for stable multi-dimensional silicon anodes, *Energy Storage Mater.*, 2025, **74**, 103911.

57 Y. Qian, Y. Chu, Z. Zheng, Z. Shadike, B. Han, S. Xiang, Y. Kang, S. Hu, C. Cao, L. Zhong, Q. Shi, M. Lin, H. Zeng, J. Wang, E. Hu, C. Weiland, X.-Q. Yang and Y. Deng, A new cyclic carbonate enables high power/low temperature lithium-ion batteries, *Energy Storage Mater.*, 2022, **45**, 14–23.

58 Y. X. Yao, N. Yao, X. R. Zhou, Z. H. Li, X. Y. Yue, C. Yan and Q. Zhang, Ethylene-carbonate-free electrolytes for rechargeable Li-ion pouch cells at sub-freezing temperatures, *Adv. Mater.*, 2022, **34**, 2206448.

59 Z. Li, Z. Li, R. Yu and X. Guo, Dual-salt poly(tetrahydrofuran) electrolyte enables quasi-solid-state lithium metal batteries to operate at −30 °C, *J. Energy Chem.*, 2024, **96**, 456–463.

60 S. Gao, K. Wang, L. Wang, X. Yang, Y. Yang, W. Xiu, X. Li and W. Lü, Concentration controlling of carboxylic ester-based electrolyte for low temperature lithium-ion batteries, *Chem.–Eur. J.*, 2024, **30**, e202401935.

61 A. Maraschky and R. Akolkar, Temperature dependence of dendritic lithium electrodeposition: A mechanistic study of the role of transport limitations within the SEI, *J. Electrochem. Soc.*, 2020, **167**, 062503.

62 W. Zhang, X. Sun, Y. Tang, H. Xia, Y. Zeng, L. Qiao, Z. Zhu, Z. Lv, Y. Zhang, X. Ge, S. Xi, Z. Wang, Y. Du and X. Chen, Lowering charge transfer barrier of $LiMn_2O_4$ *via* nickel surface doping to enhance Li^+ intercalation kinetics at subzero temperatures, *J. Am. Chem. Soc.*, 2019, **141**, 14038–14042.

63 B. Nan, L. Chen, N. D. Rodrigo, O. Borodin, N. Piao, J. Xia, T. Pollard, S. Hou, J. Zhang, X. Ji, J. Xu, X. Zhang, L. Ma, X. He, S. Liu, H. Wan, E. Hu, W. Zhang, K. Xu, X. Q. Yang, B. Lucht and C. Wang, Enhancing Li^+ transport in NMC811||Graphite lithium-ion batteries at low temperatures by using low-polarity-solvent electrolytes, *Angew. Chem., Int. Ed.*, 2022, **61**, e202205967.

64 Z. Huang, Z. Xiao, R. Jin, Z. Li, C. Shu, R. Shi, X. Wang, Z. Tang, W. Tang and Y. Wu, A comprehensive review on liquid electrolyte design for low-temperature lithium/sodium metal batteries, *Energy Environ. Sci.*, 2024, **17**, 5365–5386.

65 X.-Z. Liao, Z.-F. Ma, Q. Gong, Y.-S. He, L. Pei and L.-J. Zeng, Low-temperature performance of $LiFePO_4$/C cathode in a quaternary carbonate-based electrolyte, *Electrochem. Commun.*, 2008, **10**, 691–694.

66 K. Sun, X. Li, Z. Zhang, K. Fu, X. Xiao, L. Gong and P. Tan, Unexpected stable cycling performance at low temperatures of Li-ion batteries with Si/C anodes, *Energy Storage Mater.*, 2024, **66**, 103216.

67 G. Zhu, K. Wen, W. Lv, X. Zhou, Y. Liang, F. Yang, Z. Chen, M. Zou, J. Li, Y. Zhang and W. He, Materials insights into low-temperature performances of lithium-ion batteries, *J. Power Sources*, 2015, **300**, 29–40.

68 T. Li, Y. Cao, Q. Song, L. Peng, X. Qin, W. Lv and F. Kang, A slightly expanded graphite anode with high capacity enabled by stable lithium-ion/metal hybrid storage, *Small*, 2024, **20**, 202403057.

69 F. Lu, J. Liu, J. Xia, Y. Yang and X. Wang, Engineering C–N moieties in branched nitrogen-doped graphite tubular foam toward stable Li^+-storage at low temperature, *Ind. Eng. Chem. Res.*, 2020, **59**, 5858–5864.

70 C.-K. Ho, C.-Y. V. Li, Z. Deng, K.-Y. Chan, H. Yung and C. Yang, Hierarchical macropore-mesoporous shell carbon dispersed with $Li_4Ti_5O_{12}$ for excellent high rate sub-freezing Li-ion battery performance, *Carbon*, 2019, **145**, 614–621.

71 G. Zhao, Z. Wei, N. Zhang and K. Sun, Enhanced low temperature performances of expanded commercial mesocarbon microbeads (MCMB) as lithium ion battery anodes, *Mater. Lett.*, 2012, **89**, 243–246.

72 Y. Yan, L. Ben, Y. Zhan and X. Huang, Nano-Sn embedded in expanded graphite as anode for lithium ion batteries with improved low temperature electrochemical performance, *Electrochim. Acta*, 2016, **187**, 186–192.

73 S. Zhang, X. Ge and C. Chen, Synthesis of carbon-coated $Li_4Ti_5O_{12}$ and its electrochemical performance as anode

material for lithium-ion battery, *Chin. Chem. Lett.*, 2017, **28**, 2274–2276.

74 Y. Na, X. Sun, A. Fan, S. Cai and C. Zheng, Methods for enhancing the capacity of electrode materials in low-temperature lithium-ion batteries, *Chin. Chem. Lett.*, 2021, **32**, 973–982.

75 H. Cao, L. Wen, Z.-Q. Guo, N. Piao, G.-J. Hu, M.-J. Wu and F. Li, Application and prospects for using carbon materials to modify lithium iron phosphate materials used at low temperatures, *New Carbon Mater.*, 2022, **37**, 46–58.

76 H. Yan, J. Qian, X. Yin and F. Chen, High-energy $LiNi_{0.90}Co_{0.04}Mn_{0.03}Al_{0.03}O_2$ cathode material with lithium-reactive $Li_{0.34}La_{0.56}TiO_3$ coating and Li_2NiO_2 lithium supplying for enhanced performance lithium-ion batteries, *J. Alloys Compd.*, 2024, **976**, 173128.

77 T. Chen, J. Zhou, G. Fang, Y. Tang, X. Tan, A. Pan and S. Liang, Rational design and synthesis of $Li_3V_2(PO_4)_3$/C nanocomposites as high-performance cathodes for lithium-ion batteries, *ACS Sustainable Chem. Eng.*, 2018, **6**, 7250–7256.

78 G. Ning, S. Zhang, Z. Xiao, H. Wang and X. Ma, Efficient conducting networks constructed from ultra-low concentration carbon nanotube suspension for Li ion battery cathodes, *Carbon*, 2018, **132**, 323–328.

79 D. Xie, G. Cai, Z. Liu, R. Guo, D. Sun, C. Zhang, Y. Wan, J. Peng and H. Jiang, The low temperature electrochemical performances of $LiFePO_4$/C/graphene nanofiber with 3D-bridge network structure, *Electrochim. Acta*, 2016, **217**, 62–72.

80 S. Tan, L. Wang, L. Bian, J. Xu, W. Ren, P. Hu and A. Chang, Highly enhanced low temperature discharge capacity of $LiNi_{1/3}Co_{1/3}Mn_{1/3}O_2$ with lithium boron oxide glass modification, *J. Power Sources*, 2015, **277**, 139–146.

81 H. Dai, Y. Chen, Y. Gao, L. Gong, K. Fan, J. Zou, X. Wang, C. Zhang, M. Fu, G. Zhang, Y. Cao and C. Wang, Constructing structural isomers to reveal and enhance lithium storage in a conducting polymer, *Adv. Energy Mater.*, 2024, **14**, 2304210.

82 W. Lin, M. Zhu, Y. Fan, H. Wang, G. Tao, M. Ding, N. Liu, H. Yang, J. Wu, J. Fang and Y. Tang, Low temperature lithium-ion batteries electrolytes: Rational design, advancements, and future perspectives, *J. Alloys Compd.*, 2022, **905**, 164163.

83 H.-C. A. Shiao, D. Chua, H.-P. Lin, S. Slane and M. Salomon, Low temperature electrolytes for Li-ion PVDF cells, *J. Power Sources*, 2000, **87**, 167–173.

84 T. R. Jow, M. S. Ding, K. Xu, S. S. Zhang, J. L. Allen, K. Amine and G. L. Henriksen, Nonaqueous electrolytes for wide-temperature-range operation of Li-ion cells, *J. Power Sources*, 2003, **119**, 343–348.

85 S. Zhang, K. Xu and T. Jow, Low-temperature performance of Li-ion cells with a $LiBF_4$-based electrolyte, *J. Solid State Electrochem.*, 2003, **7**, 147–151.

86 K. Xu, S. S. Zhang, U. Lee, J. L. Allen and T. R. Jow, LiBOB: Is it an alternative salt for lithium ion chemistry?, *J. Power Sources*, 2005, **146**, 79–85.

87 S. S. Zhang, Electrochemical study of the formation of a solid electrolyte interface on graphite in a $LiBC_2O_4F_2$-based electrolyte, *J. Power Sources*, 2007, **163**, 713–718.

88 C. W. Yang, Y. H. Ren, B. R. Wu and F. Wu, Formulation of a new type of electrolytes for $LiNi_{1/3}Co_{1/3}Mn_{1/3}O_2$ cathodes working in an ultra-low temperature range, *Adv. Mater. Res.*, 2012, **455**, 258–264.

89 X. Fan, X. Ji, L. Chen, J. Chen, T. Deng, F. Han, J. Yue, N. Piao, R. Wang, X. Zhou, X. Xiao, L. Chen and C. Wang, All-temperature batteries enabled by fluorinated electrolytes with non-polar solvents, *Nat. Energy*, 2019, **4**, 882–890.

90 Y. Zhao, Z. Hu, Z. Zhao, X. Chen, S. Zhang, J. Gao and J. Luo, Strong solvent and dual lithium salts enable fast-charging lithium-ion batteries operating from −78 to 60 °C, *J. Am. Chem. Soc.*, 2023, **145**, 22184–22193.

91 W. Lv, C. Zhu, J. Chen, C. Ou, Q. Zhang and S. Zhong, High performance of low-temperature electrolyte for lithium-ion batteries using mixed additives, *Chem. Eng. J.*, 2021, **418**, 129400.

92 K. Park, S. Yu, C. Lee and H. Lee, Comparative study on lithium borates as corrosion inhibitors of aluminum current collector in lithium bis(fluorosulfonyl)imide electrolytes, *J. Power Sources*, 2015, **296**, 197–203.

93 S. Lin, H. Hua, P. Lai and J. Zhao, A multifunctional dual-salt localized high-concentration electrolyte for fast dynamic high-voltage lithium battery in wide temperature range, *Adv. Energy Mater.*, 2021, **11**, 2101775.

94 M. C. Smart, B. V. Ratnakumar, L. D. Whitcanack, K. B. Chin, S. Surampudi, H. Croft, D. Tice and R. Staniewicz, Improved low-temperature performance of lithium-ion cells with quaternary carbonate-based electrolytes, *J. Power Sources*, 2003, **119**, 349–358.

95 W. Zhang, H. Xia, Z. Zhu, Z. Lv, S. Cao, J. Wei, Y. Luo, Y. Xiao, L. Liu and X. Chen, Decimal solvent-based high-entropy electrolyte enabling the extended survival temperature of lithium-Ion batteries to −130 °C, *CCS Chem.*, 2021, **3**, 1245–1255.

96 G. Xu, X. Shangguan, S. Dong, X. Zhou and G. Cui, Formulation of blended-lithium-salt electrolytes for lithium batteries, *Angew. Chem., Int. Ed.*, 2019, **59**, 3400–3415.

97 S. S. Zhang, K. Xu and T. R. Jow, Enhanced performance of Li-ion cell with $LiBF_4$-PC based electrolyte by addition of small amount of LiBOB, *J. Power Sources*, 2006, **156**, 629–633.

98 Q. Zhao, Y. Zhang, F. Tang, J. Zhao and S. Li, Mixed salts of lithium difluoro (oxalate) borate and lithium tetrafluorobotate electrolyte on low-temperature performance for lithium-ion batteries, *J. Electrochem. Soc.*, 2017, **164**, A1873.

99 T. Zheng, J. Xiong, B. Zhu, X. Shi, Y.-J. Cheng, H. Zhao and Y. Xia, From −20 °C to 150 °C: a lithium secondary battery with a wide temperature window obtained *via* manipulated competitive decomposition in electrolyte solution, *J. Mater. Chem. A*, 2021, **9**, 9307–9318.

100 Y. Yang, Y. Chen, L. Tan, J. Zhang, N. Li, X. Ji and Y. Zhu, Rechargeable $LiNi_{0.65}Co_{0.15}Mn_{0.2}O_2$||graphite batteries operating at −60 °C, *Angew. Chem., Int. Ed.*, 2022, **61**, e202209619.

101 L. Zhang, L. Chai, L. Zhang, M. Shen, X. Zhang, V. S. Battaglia, T. Stephenson and H. Zheng, Synergistic effect between lithium bis(fluorosulfonyl)imide (LiFSI) and lithium bis-oxalato borate (LiBOB) salts in $LiPF_6$-based electrolyte for high-performance Li-ion batteries, *Electrochim. Acta*, 2014, **127**, 39–44.

102 Y. K. Liu, C. Z. Zhao, J. Du, X. Q. Zhang, A. B. Chen and Q. Zhang, Research progresses of liquid electrolytes in lithium-ion batteries, *Small*, 2022, **19**, 2205315.

103 Q. Li, G. Liu, H. Cheng, Q. Sun, J. Zhang and J. Ming, Low-temperature electrolyte design for lithium-ion batteries: Prospect and challenges, *Chem.–Eur. J.*, 2021, **27**, 15842–15865.

104 J. Holoubek, Y. Yin, M. Li, M. Yu, Y. S. Meng, P. Liu and Z. Chen, Exploiting mechanistic solvation kinetics for dual-graphite batteries with high power output at extremely low temperature, *Angew. Chem., Int. Ed.*, 2019, **131**, 19068–19073.

105 Y.-G. Cho, M. Li, J. Holoubek, W. Li, Y. Yin, Y. S. Meng and Z. Chen, Enabling the low-temperature cycling of NMC||graphite pouch cells with an ester-based electrolyte, *ACS Energy Lett.*, 2021, **6**, 2016–2023.

106 Y. Yang, P. Li, N. Wang, Z. Fang, C. Wang, X. Dong and Y. Xia, Fluorinated carboxylate ester-based electrolyte for lithium ion batteries operated at low temperature, *Chem. Commun.*, 2020, **56**, 9640–9643.

107 M. C. Smart, B. V. Ratnakumar and S. Surampudi, Electrolytes for low-temperature lithium batteries based on ternary mixtures of aliphatic carbonates, *J. Electrochem. Soc.*, 1999, **146**, 486.

108 M. Zhang, X. Lei, Y. Lv, X. Liu and Y. Ding, Reversible low temperature Li-storage in liquid metal based anodes *via* a co-solvent strategy, *Chin. J. Chem.*, 2021, **39**, 2801–2807.

109 G. Wang, H. Kang, M. Chen, K. Yan, X. Hu and E. J. Cairns, Effects of solvents on the electrochemical performance of $LiFePO_4$/C composite electrodes, *Chemelectrochem*, 2016, **4**, 376–385.

110 Y. Yin, T. Zheng, J. Chen, Y. Peng, Z. Fang, Y. Mo, C. Wang, Y. Wang, Y. Xia and X. Dong, Uncovering the function of a five-membered heterocyclic solvent-based electrolyte for graphite anode at subzero temperature, *Adv. Funct. Mater.*, 2023, **33**, 2215151.

111 J. Ming, Z. Cao, Y. Wu, W. Wahyudi, W. Wang, X. Guo, L. Cavallo, J.-Y. Hwang, A. Shamim, L.-J. Li, Y.-K. Sun and H. N. Alshareef, New insight on the role of electrolyte additives in rechargeable lithium ion batteries, *ACS Energy Lett.*, 2019, **4**, 2613–2622.

112 H. Li, J. Cai, J. Liao, Y. Li, X. Zeng, X. He, W. Fan, C. Fan, Z. Ma and J. Nan, A functional electrolyte containing propyl 4-methylbenzene sulfonate (PMBS) additive to improve the cycling performance of the $LiNi_{0.8}Co_{0.1}Mn_{0.1}O_2$/graphite full cell under the low temperature of −10 °C, *J. Mater. Chem. A*, 2023, **11**, 24970–24981.

113 Y. Yang, Y. Li, J. Zhang, X. Liu, H. Yu, L. Wu, C. Duan, Z. Xi, R. Fang and Q. Zhao, Co-Intercalation-free graphite anode enabled by an additive regulated interphase in an ether-based electrolyte for low-temperature lithium-ion batteries, *ACS Appl. Mater. Interfaces*, 2024, **16**, 10116–10125.

114 N. Qin, J. Chen, Y. Lu, Y. Li, W. Cai, J. Li, C. Zhang, Z. Chen, J. P. Zheng and L. Jin, Trace $LiBF_4$ enabling robust LiF-rich interphase for durable low-temperature lithium-ion pouch cells, *ACS Energy Lett.*, 2024, **9**, 4843–4851.

115 Z. Han, D. Zhang, H. Wang, G. Zheng, M. Liu and Y. He, Research progress and prospect on electrolyte additives for interface reconstruction of long-life Ni-rich lithium batteries, *Acta Phys.–Chim. Sin.*, 2024, **40**, 2307034.

116 O. Matsuoka, A. Hiwara, T. Omi, M. Toriida, T. Hayashi, C. Tanaka, Y. Saito, T. Ishida, H. Tan, S. S. Ono and S. Yamamoto, Ultra-thin passivating film induced by vinylene carbonate on highly oriented pyrolytic graphite negative electrode in lithium-ion cell, *J. Power Sources*, 2002, **108**, 128–138.

117 J. Xu, W. Yao, Y. Yao, Z. Wang and Y. Yang, Effect of fluoroethylene carbonate additive on the performance of lithium ion battery, *Acta Phys.–Chim. Sin.*, 2009, **25**, 201.

118 C. Zhu, W. Lv, J. Chen, C. Ou, Q. Zhang, H. Fu, H. Wang, L. Wu and S. Zhong, Butyl acrylate (BA) and ethylene carbonate (EC) electrolyte additives for low-temperature performance of lithium ion batteries, *J. Power Sources*, 2020, **476**, 228697.

119 R. Guo, Y. Che, G. Lan, J. Lan, J. Li, L. Xing, K. Xu, W. Fan, L. Yu and W. Li, Tailoring low-temperature performance of a lithium-ion battery *via* rational designing interphase on an anode, *ACS Appl. Mater. Interfaces*, 2019, **11**, 38285–38293.

120 L. Li, W. Lv, J. Chen, C. Zhu, S. Dmytro, Q. Zhang and S. Zhong, Lithium difluorophosphate ($LiPO_2F_2$): An electrolyte additive to help boost low-temperature behaviors for lithium-ion batteries, *ACS Appl. Energy Mater.*, 2022, **5**, 11900–11914.

121 X. Yang, Y. Huang, J. Li, W. Huang, W. Yang, C. Wu, S. Tang, F. Ren, Z. Gong, N. Zhou and Y. Yang, Understanding of working mechanism of lithium difluoro(oxalato) borate in Li||NCM85 battery with enhanced cyclic stability, *Energy Mater.*, 2023, **3**, 300029.

122 J. Qin, Y. Zhao, X. Meng, M. Wang, Z. Song, X. Ai and H. Zhan, Amphiphilic molecule-assisted perfluoro-alkanes electrolyte for low temperature lithium metal batteries, *Chem. Eng. J.*, 2024, **496**, 153818.

123 F. Ren, Z. Li, J. Chen, P. Huguet, Z. Peng and S. Deabate, Solvent–diluent interaction-mediated solvation structure of localized high-concentration electrolytes, *ACS Appl. Mater. Interfaces*, 2022, **14**, 4211–4219.

124 J. Holoubek, K. Kim, Y. Yin, Z. Wu, H. Liu, M. Li, A. Chen, H. Gao, G. Cai, T. A. Pascal, P. Liu and Z. Chen, Electrolyte design implications of ion-pairing in low-temperature Li metal batteries, *Energy Environ. Sci.*, 2022, **15**, 1647–1658.

125 X. Zhang, L. Zou, Y. Xu, X. Cao, M. H. Engelhard, B. E. Matthews, L. Zhong, H. Wu, H. Jia, X. Ren, P. Gao, Z. Chen, Y. Qin, C. Kompella, B. W. Arey, J. Li, D. Wang, C. Wang, J. G. Zhang and W. Xu, Advanced electrolytes for fast-charging high-voltage lithium-ion batteries in wide-temperature range, *Adv. Energy Mater.*, 2020, **10**, 2000368.

126 L. L. Jiang, C. Yan, Y. X. Yao, W. Cai, J. Q. Huang and Q. Zhang, Inhibiting solvent co-intercalation in a graphite anode by a localized high-concentration electrolyte in fast-charging batteries, *Angew. Chem., Int. Ed.*, 2020, **60**, 3402–3406.

127 N. Piao, J. Wang, X. Gao, R. Li, H. Zhang, G. Hu, Z. Sun, X. Fan, H.-M. Cheng and F. Li, Designing temperature-insensitive solvated electrolytes for low-temperature lithium metal batteries, *J. Am. Chem. Soc.*, 2024, **146**, 18281–18291.

128 X. Liu, J. Zhang, X. Yun, J. Li, H. Yu, L. Peng, Z. Xi, R. Wang, L. Yang, W. Xie, J. Chen and Q. Zhao, Anchored weakly-solvated electrolytes for high-voltage and low-temperature lithium-ion batteries, *Angew. Chem., Int. Ed.*, 2024, **63**, e202406596.

129 T. Ma, Y. Ni, Q. Wang, W. Zhang, S. Jin, S. Zheng, X. Yang, Y. Hou, Z. Tao and J. Chen, Optimize lithium deposition at low temperature by weakly solvating power solvent, *Angew. Chem., Int. Ed.*, 2022, **134**, e202207927.

130 S. Chen, J. Zheng, D. Mei, K. S. Han, M. H. Engelhard, W. Zhao, W. Xu, J. Liu and J. G. Zhang, High-voltage lithium-metal batteries enabled by localized high-concentration electrolytes, *Adv. Mater.*, 2018, **30**, 1706102.

131 T. Feng, G. Yang, S. Zhang, Z. Xu, H. Zhou and M. Wu, Low-temperature and high-voltage lithium-ion battery enabled by localized high-concentration carboxylate electrolytes, *Chem. Eng. J.*, 2022, **433**, 134138.

132 T. N. Tran, X. Cao, Y. Xu, P. Gao, H. Zhou, F. Guo, K. S. Han, D. Liu, P. M. L. Le, J. M. Weller, M. H. Engelhard, C. Wang, M. S. Whittingham, W. Xu and J. G. Zhang, Enhancing cycling stability of lithium metal batteries by a bifunctional fluorinated ether, *Adv. Funct. Mater.*, 2024, **34**, 2407012.

133 P. Lai, X. Deng, Y. Zhang, J. Li, H. Hua, B. Huang, P. Zhang and J. Zhao, Bifunctional localized high-concentration electrolyte for the fast kinetics of lithium batteries at low temperatures, *ACS Appl. Mater. Interfaces*, 2023, **15**, 31020.

134 Z. Cao, X. Zheng, M. Zhou, T. Zhao, L. Lv, Y. Li, Z. Wang, W. Luo and H. Zheng, Electrolyte solvation engineering toward high-rate and low-temperature silicon-based batteries, *ACS Energy Lett.*, 2022, **7**, 3581–3592.

135 Y. Yang, Z. Fang, Y. Yin, Y. Cao, Y. Wang, X. Dong and Y. Xia, Synergy of weakly-solvated electrolyte and optimized interphase enables graphite anode charge at low temperature, *Angew. Chem., Int. Ed.*, 2022, **61**, e202208345.

136 C. Liu, Z. Li, L. Jiang, H. Zhu, F. Wang and L. Sheng, Dipole-dipole interactions in electrolyte to facilitate Li-ion desolvation for low-temperature Li-ion batteries, *J. Energy Chem.*, 2025, **104**, 678–686.

137 Y. Yang, D. M. Davies, Y. Yin, O. Borodin, J. Z. Lee, C. Fang, M. Olguin, Y. Zhang, E. S. Sablina, X. Wang, C. S. Rustomji and Y. S. Meng, High-efficiency lithium-metal anode enabled by liquefied gas electrolytes, *Joule*, 2019, **3**, 1986–2000.

138 Y. Yang, Y. Yin, D. M. Davies, M. Zhang, M. Mayer, Y. Zhang, E. S. Sablina, S. Wang, J. Z. Lee, O. Borodin, C. S. Rustomji and Y. S. Meng, Liquefied gas electrolytes for wide-temperature lithium metal batteries, *Energy Environ. Sci.*, 2020, **13**, 2209–2219.

139 S. Xu, Z. Sun, C. Sun, F. Li, K. Chen, Z. Zhang, G. Hou, H. M. Cheng and F. Li, Homogeneous and fast ion conduction of PEO-based solid-state electrolyte at low temperature, *Adv. Funct. Mater.*, 2020, **30**, 2007172.

140 J. Park, H. Seong, C. Yuk, D. Lee, Y. Byun, E. Lee, W. Lee and B. J. Kim, Design of fluorinated elastomeric electrolyte for solid-state lithium metal batteries operating at low temperature and high voltage, *Adv. Mater.*, 2024, **36**, 2403191.

141 D. M. Davies, Y. Yang, E. S. Sablina, Y. Yin, M. Mayer, Y. Zhang, M. Olguin, J. Z. Lee, B. Lu, D. Damien, O. Borodin, C. S. Rustomji and Y. S. Meng, A safer, wide-temperature liquefied gas electrolyte based on difluoromethane, *J. Power Sources*, 2021, **493**, 229668.

142 Y. Yin, J. Holoubek, A. Liu, B. Sayahpour, G. Raghavendran, G. Cai, B. Han, M. Mayer, N. B. Schorr, T. N. Lambert, K. L. Harrison, W. Li, Z. Chen and Y. S. Meng, Ultralow-temperature Li/CF_x batteries enabled by fast-transport and anion-pairing liquefied gas electrolytes, *Adv. Mater.*, 2022, **35**, 2207932.

143 J. Xiang, Y. Zhang, B. Zhang, L. Yuan, X. Liu, Z. Cheng, Y. Yang, X. Zhang, Z. Li, Y. Shen, J. Jiang and Y. Huang, A flame-retardant polymer electrolyte for high performance lithium metal batteries with an expanded operation temperature, *Energy Environ. Sci.*, 2021, **14**, 3510–3521.

144 X. Liu, D. Wang, Z. Zhang, G. Li, J. Wang, G. Yang, H. Lin, J. Lin, X. Ou and W. Zheng, Gel polymer electrolyte enables low-temperature and high-rate lithium-ion batteries *via* bionic interface design, *Small*, 2024, **20**, 2404879.

145 X. Ren, L. Zou, S. Jiao, D. Mei, M. H. Engelhard, Q. Li, H. Lee, C. Niu, B. D. Adams, C. Wang, J. Liu, J.-G. Zhang and W. Xu, High-concentration ether electrolytes for stable high-voltage lithium metal batteries, *ACS Energy Lett.*, 2019, **4**, 896.

146 Y. Zhang, S. Li, J. Shi, J. Lai, Z. Zhuang, J. Liu, W. Yang, L. Ma, Y.-P. Cai, J. Xu and Q. Zheng, Revealing the key role of non-solvating diluents for fast-charging and low temperature Li-ion batteries, *J. Energy Chem.*, 2024, **94**, 171–180.

147 G. Song, Z. Yi, F. Su, L. Xie, Z. Wang, X.-X. Wei, G. Xu and C.-M. Chen, Boosting the low-temperature performance for Li-ion batteries in $LiPF_6$-based local high-concentration electrolyte, *ACS Energy Lett.*, 2023, **8**, 1336.

148 L. Luo, K. Chen, R. Cao, H. Chen, M. Xia, A. Zhao, X. Chen, W. Chen, Z. Chen, Y. Fang and Y. Cao, Ethyl fluoroacetate with weak Li^+ interaction and high oxidation resistant induced low-temperature and high-voltage graphite// $LiCoO_2$ batteries, *Energy Storage Mater.*, 2024, **70**, 103438.